[AMERICAN JOURNAL OF SCIENCE, VOL. 294, SUMMER, 1994, P. 802–860]

KINEMATICS OF BASEMENT-INVOLVED COMPRESSIVE STRUCTURES*

WAYNE NARR** and JOHN SUPPE
Department of Geological and Geophysical Sciences
Guyot Hall, Princeton University
Princeton, NJ 08544

ABSTRACT. Low-temperature, basement-involved compressive folds are confined largely to the hanging walls of thrust faults and appear to be produced in response to both propagation and slip on non-planar faults. In this paper we develop a simple, two-dimensional, kinematic theory of basement-involved structures capable of predicting much of their geometric complexity and diversity. The theory is tested by applying it in the construction of retrodeformable cross sections and sequential kinematic models of three structures—Willow Creek anticline, Big Thompson anticline, and a small monocline on Casper Mountain—as well as less rigorous comparison with several other well-constrained structures.

Thrust faults commonly propagate through the brittle upper crust along non-planar paths due to interaction with inhomogeneities such as preexisting faults or other zones of weakness, rock anisotropy, and/or effects of spacial or temporal stress field variability. The folding associated with displacement on such a complex system of basement faults reduces conceptually to the behavior of a system of *fault-fault-fold triple junctions*.

A second key aspect of basement-involved structures is the response of the stratified cover sequence in the evolving basement structure. The main monocline in the stratified cover in many cases forms as a *drape fold* over a triple junction in the basement. The model proposed here presents a complex kinematic history for drape fold development. Layer-parallel shortening is predicted for the cover sequence of many triple junctions during early stages of deformation, whereas at later stages the cover experiences layer-parallel extension, especially in the steep limb and beneath the propagating fault. The cover strata in the steep limbs of monoclines we studied exhibit different stages in such a kinematic sequence: (1) layer-parallel shortening with smaller-scale compressional folds (Rattlesnake Mountain anticline, Bighorn Mountains, and Casper Mountain); (2) wedging (Willow Creek anticline); and (3) layer-parallel extension (Big Thompson anticline, Rattlesnake Mountain anticline, and Banner Mountain).

INTRODUCTION

Low-temperature, basement-involved, compressive structures, such as those in the eastern Rocky Mountains in the United States, are typically monoclines that show complex, often confusing kinematic histories. For example Wise (1963), in describing the Owl Creek Mountains of Wyo-

* This paper is in a sense an extended response to Rodgers' (1987) summary of basement-involved structures world-wide, giving a conceptual framework for the diversity that he documents.

** Present Address: Chevron Overseas Petroleum Inc., 6001 Bollinger Canyon Road, San Ramon, California 94583.

ming, pointed out "a seeming inconsistency, the presence of both normal and thrust faults of almost the same age in the same (structural) environment." Likewise, Avouac, Beyer, and Tapponnier (1992) show that both normal and thrust faults were activated during recent earthquake activity along the basement-involved El Asnam fault in the Atlas mountains of North Africa. Such "seeming inconsistencies" as well as a high degree of structural diversity are hallmarks of basement-involved structures and present challenges that need to be addressed by any model of such structures.

Obtaining an accurate general picture of even the present deformed geometry of basement-involved structures is difficult because of their complexity and diversity combined with the fact that individual structures are so large that some crucial elements of their geometry are nearly always hidden. A suite of well exposed basement-involved structures was studied to understand better their characteristic geometry, kinematic history, and deformational processes. These data have been used to develop a quantitative kinematic model that describes the development of basement-involved structures. This paper describes the kinematic model, discusses the geometries of six of the structures that helped inspire the model, and applies the model to interpret the kinematic development of three structures.

Kinematic structural models such as the fault-bend and fault-propagation fold models (Suppe, 1983; Jamison, 1987; Chester and Chester, 1990; Suppe and Medwedeff, 1990; Mitra, 1993) provide quantitative relationships between fault shape and fold shape that are being used to interpret successfully the geometry and kinematic histories mainly of thin-skinned fold-and-thrust belts (for example, Medwedeff, 1992; Mount, Suppe, and Hook, 1990; Suppe, Chou, and Hook, 1991). These models are based on the requirement that any viable structural interpretation must be retrodeformable; that is, an interpretation is viable only if it can be returned to an undeformed state in which all mass is accounted for and where each step of the deformation process is physically reasonable. To date, no such model has proven generally useful for interpretation of basement-involved structures.

Although several recent quantitative models for basement-involved structures have been advanced (Cook, 1988; Erslev, 1991), they approach the problem mainly from the standpoint of homogeneous area balancing. As such, their approach to the problem differs from the viewpoint taken in this paper; we seek a more fully constrained relationship between fault shape, fold shape, and kinematic history.

This paper presents a new kinematic model of the development of basement-involved structures—based on an extension of fault-bend folding theory (Suppe, 1983)—and discusses the motivating field observations. The model is based on the kinematics of area-constant (volume-constant in 3D) fault-fault-fold triple junctions. Many of the complexities of basement-involved structures, for example the common presence of steep near-surface faults in conjunction with moderately dipping deeper

faults, the existence of rotated basement in some structures but not others, and the change in vergence along strike exhibited by some basement uplifts, can be explained with simple triple-junction geometric elements or by linking together several triple junctions to construct more complex structures.

Like all models, the triple junction model is a hypothesis. The first part of this paper presents this hypothetical model. In the latter and longer portion of the paper, we test the model by applying it in the interpretation of a number of well-exposed basement-involved structures. Because the model appears to stand up successfully both to qualitative and quantitative application, we feel the observational basis of the model is herein established.

The triple-junction model is motivated by the understanding that basement contains substantial preexisting structure that is reactivated during younger crustal compression. As a thrust fault propagates through to the brittle upper crust, it may encounter various preexisting weak surfaces such as faults, deep joints, or lithological boundaries which are generally oblique to the propagating fault. If slip initiates on any of these preexisting structures a fault-fault-fold triple junction will initiate through the process of fault-bend folding. We envisage basement-involved structures as being produced by slip on fault systems composed of a number of fault-fault-fold triple junctions localized by preexisting structure. Furthermore, we imagine that some preexisting structures may be oblique to the tectonic compression and may slip with an oblique or strike-slip component to the faulting. However, we consider here only two-dimensional, dip-slip deformation.

Background on Basement-Involved Structures

The importance of better understanding the kinematic development of basement-involved structures can be gauged by their widespread occurrence. They are perhaps best known and best studied in the Laramide eastern Rocky Mountains of the United States because of their often-excellent surface exposures and extensive petroleum data; however, basement-involved structures are widely developed on all continents (Rodgers, 1987). Table 1 is a sampling—by no means exhaustive—of orogenic belts in which basement-involved structures are an important constituent, listed by major crustal plate. Furthermore basement-involved structures have been interpreted to exist on Mars, the Moon, and Venus based on imagery and altimetry obtained from spacecraft (Golombek and others, 1990; Golombek, Plescia, and Franklin, 1991; Suppe and Narr, 1989).

Basement-involved structures that formed at somewhat higher temperatures—near the brittle-plastic transition, commonly about low greenschist facies—are found in the hinterland of many orogenic belts, and their geometry appears qualitatively similar to lower-temperature structures. For example, the Taconic basement massifs of the Appalachians (Stanley and Armstrong, 1988) and the lower temperature Alpine base-

TABLE 1

Some orogenic belts where low-temperature, basement-involved, compressive structures are known

Orogenic Belt	Deformation Age	Reference
North American Plate		
Boothia-Cornwallis	Devonian	Kerr, 1977; Okulitch, Packard, and Zolnai, 1986
Ancestral Rocky Mountains (including Arbuckle and Wichita Mtns.)	Pennsylvanian	Blythe, Sugar, and Phipps, 1988; Mallory, 1972
Eastern Rocky Mountains	Paleogene	Berg, 1962; Cross, 1986
Transverse Ranges	Neogene	Sylvester and Smith, 1979; Dibblee, 1982
South American Plate		
Venezuelian Andes, Sierra de Perija, and Santa Marta Massif	Neogene	Kellogg and Bonini, 1982; Meier, Schwander, and Laubscher, 1987
Central Cordillera (Colombia)	Neogene	Butler and Schamel, 1988
Eastern Cordillera (Colombia)	Neogene	Julivert, 1970; Dengo and Covey, 1993
Eastern Cordillera and Subandean Lowland (Peru)	Neogene	Sebrier, and others, 1988; Barazangi and Isacks, 1979
Sierras Pampeanas (Argentina)	Neogene	Allmendinger, and others, 1983
Caribbean Plate		
Trinidad and Tobago	Neogene	Robertson and Burke, 1989
African Plate		
Western High Atlas	Jurassic to Recent	Froitzheim, Stets, and Wurster, 1988
Central High Atlas	Tertiary	Fraissinet and others, 1988
Cape Ranges	Late Pz. to Triassic	Rodgers, 1987
Witwatersrand Basin	Archean	Myers McCarthy, and Stanistreet, 1989
Eurasian Plate		
Harz Mountains	Late Cretaceous	Rodgers, 1987
Pyrenees Mountains	Paleogene	Williams and Fischer, 1984; Choukroune, 1989
Zagros Mountains	Neogene	Jackson and Fitch, 1981; Molnar and Chen, 1983
Tien Shan	Neogene	Tapponnier and Molnar, 1979; Molnar and Chen, 1983
Central Sumatra Basin	Neogene	Eubank and Makki, 1981
Indian-Australian Plate		
New Guinea fold-and-thrust belt	Neogene	Abers and McCaffrey, 1988
Ngalia Basin, Australia	Carboniferous	Wells, Moss, and Sabitay, 1972

ment massifs (Trumpy, 1980) share many features with the basement-involved structures of the eastern Rockies, and the kinematics of their development may be analogous. Nevertheless, we are only considering brittle structures in this paper.

Stone (1984) presents an encapsulation of conceptual thinking about basement-involved structures by showing a history of interpretations of the structure of Rattlesnake Mountain, Wyoming. He shows six cross sections by different authors based entirely on surface data, which reflect changing ideas without any appreciable differences in available data.

Different ideas about basement-involved structures have centered around three key considerations: (1) geometry of the main causative fault; (2) mechanical behavior of the basement rock; and (3) the response of the stratified cover to the deformation.

Geometry of the main causative fault: Most geologists agree that basement-involved structures form in response to displacement on a fault or relatively narrow fault zone that cuts through the basement and dissipates upward into the cover (but see also Spang, Evans, and Berg, 1985). Ideas about the shape and dip of the main fault have varied. Relatively early mapping and regional studies in the eastern Rockies show interpretations with planar or listric thrust faults of moderate dip (Beckwith, 1941; Thom, 1955). However, steep faults are seen commonly at the cover-basement contact in the steeply-dipping limbs of basement-involved structures; this observation stimulated the interpretation of primarily vertical movement of the crust along near-vertical faults (Stearns, 1971; Matthews, 1978). Concave-downward faults, which are vertical in the basement but become shallowly-dipping in the cover, were also proposed as a general feature of basement-involved structures (Wise, 1963; Prucha, Graham, and Nicholson, 1965).

Geophysical and well data have placed important constraints on fault geometry. Early gravity and well data showed important evidence for moderately dipping faults (Berg, 1962; Berg and Romberg, 1966). More recently seismic profiles and deep drilling of a number of basement uplifts, for example the Wind River Mountains of Wyoming, document moderately-dipping master faults for many but not all these structures (Smithson and others, 1978; Gries, 1983; Gries and Dyer, 1985). It is apparent that many basement-involved structures form in response to crustal compression. Kinematic indicators associated with the structures we studied lead to the same conclusion (Narr, ms and 1993).

Mechanical behavior of the basement rock: The mechanical response of basement during development of basement-involved structures has been a topic of considerable debate. Some workers present evidence that basement sustains no internal strain but deforms only by movement of rather large, rigid blocks (Prucha, Graham, and Nicholson, 1965; Stearns, 1971; Matthews, 1986; Erslev, Rogers, and Harvey, 1988). In contrast workers have argued on the basis of the overall geometry of basement-involved structures that the crystalline basement must experience relatively continuous folding (Berg, 1962; Blackstone, 1983; Brown, 1984). Narr (1993) shows that both these endmembers exist; some structures show folding of the basement, whereas in other structures the basement is translated rigidly, showing no evidence of folding.

Deformational response of the stratified cover: The stratified, generally less cohesive cover of basement-involved structures is commonly somewhat detached mechanically from the basement, especially in the steep limb. Stearns (1971) and Stearns and Jamison (1977) demonstrate thinning of the cover in the steep limb of Rattlesnake Mountain anticline, Wyoming, and in several areas along a major uplift in Colorado National Monument. Likewise, Stone (1983) shows extension of strata in the steep

limb of Elk Basin anticline. However, other structures show thickening in the steep limb by compressive faulting or folding, such as the "rabbit-ear" folds of Brown (1984), duplication of strata (Lowell, 1985, p. 166, southeast-plunging nose of Rattlesnake Mountain anticline), and wedging in the steep limb (Perry and others, 1988, Grand Hogback monocline, Colorado). Still others document both layer parallel shortening and extension in the steep limbs of basement-involved structures (Spang, Evans, and Berg, 1985, Sage Creek anticline, Wyoming; Hennings and Spang, 1987, Dry Fork Ridge anticline, Wyoming).

In the following section we present a kinematic model that provides a unified conceptual framework to explain the diverse kinematic development of basement-involved structures. This model is tested in later sections of this paper by applying it to explain the quantitative kinematic development of three geometrically well-constrained basement-involved structures and compared qualitatively with several additional structures.

KINEMATIC MODEL OF BASEMENT-INVOLVED STRUCTURES

Based on the above discussion, any theory must address the following characteristics of basement-involved structures—in addition to the general characteristics of heterogeneity and diversity:

1. Basement-involved structures are commonly monoclines.
2. The structures commonly form above a contractional fault in the basement.
3. The basement behaves as a rigid block in some structures, but in others it is folded.
4. The main fault can disappear as it proceeds up into the cover sequence.
5. The steep limbs of folds commonly form by the cover draping over a faulted edge of basement as the hanging wall is uplifted.
6. Deformation in the cover is concentrated in the steep limb and can involve both layer-parallel shortening and layer-parallel extension.

The first three characteristics bear on the behavior of the basement and the geometry of the deep fault, whereas the last three bear on the cover and its interaction with the basement.

Within this section of the paper we first present an example of a kinematic model of basement-involved structures which allows us to introduce some of the key properties of such models—we consider it a "working prototype." Second we discuss the substantial diversity of fault-fault-fold triple-junction behavior that is possible in basement rocks. Finally we present the quantitative triple-junction theory, which is used to construct both the models and the retrodeformable cross sections of this paper.

Prototypical Kinematic Model

Figure 1 is a simple retrodeformable kinematic model that shows many of the characteristics of basement-involved structures. The model is composed of a fault-fault-fold triple junction in the basement, initially at point t^*, with an overlying horizontally layered cover sequence (fig. 1A).

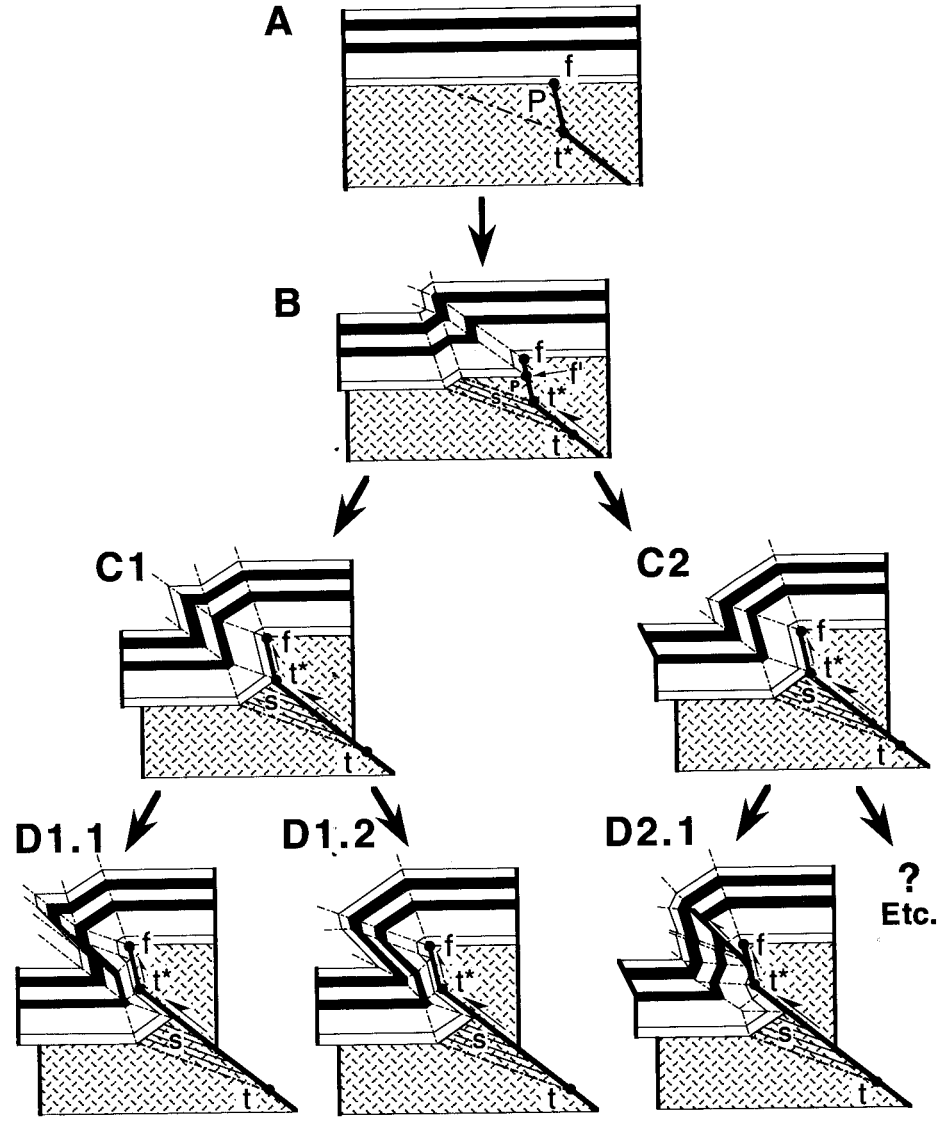

Fig. 1. Model of the sequential kinematic development of a basement-involved compressive structure. Point t^* is a triple junction that moves up along with the hanging wall, causing an active axial surface to sweep up through the prism P. Stages **A** to **C** show layer-parallel shortening in the cover; stage **D** shows layer-parallel extension. Details of deformation in the cover are not uniquely predicted by the model, hence stages **C** and **D** illustrate several possibilities.

Note that its initial state (1A) is *kinematically* capable of leading to a variety of final structures (D1.1, D1.2, D2.1, . . . et cetera), depending on how the cover is able to respond to the displacements of the basement. No unique kinematic solution exists for the forward problem.

Kinematics of the basement.—The lower fault bifurcates at its upper terminus, point t^*, forming a steeper-dipping fault and a gently dipping axial surface (dashed) that bound a triangle of rock in the basement, region P (fig. 1A). This steeper fault could be, for example, a preexisting zone of weakness about to be reactivated or the upper segment of a listric proto-fault. As the fault begins to slip, point t^*, which is attached to the hanging wall, separates from the corresponding point t in the footwall. An active axial surface travels with t^*, folding the rock as it sweeps through triangle P ("P" for prism in a 3D structure; fig. 1B). An inactive axial surface is attached to the footwall cutoff t, marking the initial location of the active axial surface (fig. 1A). The area of rock through which the active axial surface has swept is labeled S (for "sheared") in figure 1. In figure 1C, t^* has just reached the uppermost point in the basement footwall; after this stage the hanging wall slips forward without further interaction with the basement footwall[1] (fig. 1D). Point t^* is a fault-fault-fold triple junction. It can be treated kinematically like the triple junctions of plate tectonics, except that all our triple junctions conserve surface area.

Although the model shows region S undergoing penetrative, uniform shearing in response to axial surface migration, this is a generalization of the kinematic response. In actual structures more complex deformation would be expected here. Rotation and/or displacement of unsheared basement blocks along discrete faults, such as the footwall structures discussed by Watkinson (1993), may develop in this part of the structure.

Kinematics of the cover.—A discontinuity in deformation exists across the cover-basement contact in our prototypical model because (1) layer thickness and bed length are conserved in the cover strata wherever possible, which causes the folds to change orientation across the contact; (2) the length of the basement-cover contact changes as a result of folding in the basement, causing a detachment to form (figs. 1B–D); and (3) the steep basement fault terminates at the basement-cover contact (point f in fig. 1).

It is important to bear in mind that the triple-junction model predicts the kinematics of the cover in a general way—for example, extension or shortening. The details of how this is accomplished will be different in different structures. Figure 1 shows a limited set of possible responses of the cover sequence to the evolving basement-involved structure.

[1] While this paper was in review a major paper on kinematic modelling of inversion structures by Mitra (1993) appeared, and it also shows triple-junction-based fault-related folding of the footwall.

1. *Folds in the cover:* The axial surfaces bounding deformed region *S* refract to a steeper dip in the cover to bisect the angle between fold limbs and hence satisfy the requirement of conservation of layer thickness. Furthermore, a second fold is created as a result of the increased length of basement-cover contact created as the hanging-wall basement block protrudes into the cover in figure 1C.1.

Secondary axial surfaces are created in the cover as a result of interference of two kink bands, as seen in figure 1C.1. The two axial surfaces that emanate from the synclinal bends in the basement surface intersect within the cover to form a single axial surface at the level of the lower black layer. The total layer-parallel simple shear produced by the more open folds associated with the two merging axial surfaces is less than the shear produced by the resultant, tighter fold (Suppe, 1983; see also fig. 9-9 in Suppe, 1985). This produces an imbalance of layer-parallel simple shear. This increase of shear strain is consumed in the creation of the flat-topped anticline at the top of the steep limb, which originates at the same stratigraphic level at which the two synclinal axial surfaces merge. This is, in effect, the "out-of-syncline volume problem" discussed by Brown (1984), and the small anticline in the steep limb of figure 1C is kinematically analogous to one of his "rabbit-ear folds."

Alternatively, the "excess" bed length that can lead to the development of rabbit-ear folds may form subsidiary structures in a different location on the main structure or be transferred out of the local structure by layer-parallel shear, as in figure 1C.2.

2. *Basement-cover detachment:* Slip along the basement-cover contact is required because of changes in length associated with folding and with protrusion of basement blocks into the cover. In our prototypical example protrusion increases the length of the contact (fig. 1D) whereas folding decreases the length (fig. 1C). The length of the basement-cover interface of the top of triangle *P* in figure 1A decreases as the active axial surface sweeps through it, until it reaches a minimum length when *P* becomes completely deformed to triangle *S* when triple junction t^* reaches the basement-cover contact (fig. 1C). As the length of the basement surface decreases, the cover must either be displaced, as shown by the offset at the left side of the model in figure 1, B to D, or the cover must undergo additional folding or faulting.

The main anticline in the cover develops over the faulted edge of the rigid basement hanging wall block, which we refer to as a *drape anticline* (following Prucha, Graham, and Nicholson, 1965). Such folds have also been referred to as forced folds (Stearns, 1978).

The steep fault between basement and cover that terminates at point *f* is here called a *drape-induced detachment,* because the basement is unfolded, and the fault runs parallel to bedding in the cover rocks. As slip accumulates the steep kink band widens, with the active axial surface terminating at point f' and the inactive axial surface at *f* (fig. 1B). The detachment does not exist to the right of point *f*, only an unconformity. Note that the detachment is actively slipping only to the left of point f';

the steep detachment between f and f' is always inactive. The basement rock that is missing across the steep drape-induced detachment lies within the upper part of triangle S. The drape-induced detachment is produced by the downward withdrawal of the wedge of material S (P in the undeformed state). All the case studies we present later in this report appear to have steep, drape-induced detachments.

Changes in kinematics of the cover.—As deformation proceeds beyond the stage of figure 1C new basement surface, below t^*, is created at a rate equal to the fault slip (fig. 1D). At this stage in the deformation, strata low in the cover sequence of the example shown in figure 1D.1 are stretched and thinned within the steep limb and beneath the moderately-dipping fault at the base of the hanging wall. In one model scenario the thinning occurs beneath the level of the rabbit-ear fold (fig. 1D.1.1). In the other scenario the rabbit-ear fold that formed in the earlier stages of development is consumed as strata in the steep limb are stretched (fig. 1D.1.2).

In the alternative scenario, illustrated in figure 1C.2, no thinning occurs in the steep limb of the drape anticline, but an extension fault cuts the lower stratigraphic units, while an additional axial surface emerges from the upper end of the extension fault, bending the strata downward in advance of the propagating extension fault.

The deformational sequence of the cover in figure 1 is qualitatively similar to that of many basement-involved structures, and it shows two basic stages. The early stage of development (fig. 1A–C) of the structure is accompanied by overall layer-parallel shortening. The later stage of development (following fig. 1C) is characterized by overall extension of the cover. Extension in the cover increases with increased displacement on the main fault. The magnitude of extension in the cover at this later stage of deformation is dependent on stratigraphic level. Horizons higher than those illustrated in figure 1D would still be undergoing layer-parallel shortening. The thinned and overturned beds that occur sometimes beneath the main thrust (the "fault sliver" of Gries, 1983) of many basement-involved structures that have relatively large fault slip are formed during the extensional phase (fig. 1D).

The magnitudes of extension and shortening in the cover depend on the geometry of the basement triple junction. For example, if the lower fault segment in figure 1 were steeper, the shortening of the upper edge of triangle P would be less, and production of new basement surface by edge protrusion would be greater. The net shortening of the basement surface would be less during the early stage of development of the structure. This deformational sequence in the cover, layer parallel shortening followed by extension, is the same general deformational sequence proposed in the trishear model of Erslev (1991).

The deformation in the cover of actual structures will differ in detail from the prototypical model of figure 1. That is why we have shown several alternative structures in the cover for the same triple-junction migration in the basement; the structural response of the cover is non-unique.

Other Triple-Junction Models

The prototypical model of figure 1 is based on a fault-fault-fold triple junction t^* that moves with the hanging wall. A variety of triple-junction models are possible; for example, the concave fault bend at the base of a thrust ramp normally generates a fault-fault-fold triple junction that is fixed to the footwall. There are in general three stable triple-junction configurations: *fault-fault-fold, fault-fold-fold,* and *fold-fold-fold.* The only other possibility is a *fault-fault-fault* triple junction, but this configuration is unstable and can exist only instantaneously. In this paper we concentrate on fault-fault-fold triple junctions, because they are the most important for natural structures in the brittle upper crust.

Fault-fault-fold triple junctions can be subdivided into two groups based on whether the angular distribution of the three branches (faults or axial surfaces) are distributed through a range of (1) more than 180° (fig. 2A–C), or (2) less than 180° (fig. 2D–F). These models are drawn from the perspective that an input displacement along branch 1 produces a kinematic response along branches 2 and 3. These triple junctions are stable configurations for which the sense of displacement would produce compressive structures.

The input displacements of figure 2C and F occur along axial surfaces, which may link downward with other structures that generate upward-continuing axial surfaces, such as one of the other four permissible triple junctions. Alternatively these fold-driven models may be geologically important in the context of deeper crustal processes and may be applicable, for example, in linking ductile deformation in the lower crust with brittle deformation in the upper crust (Ramsay, 1980). In the rest of this discussion we will only consider fault-driven triple junctions

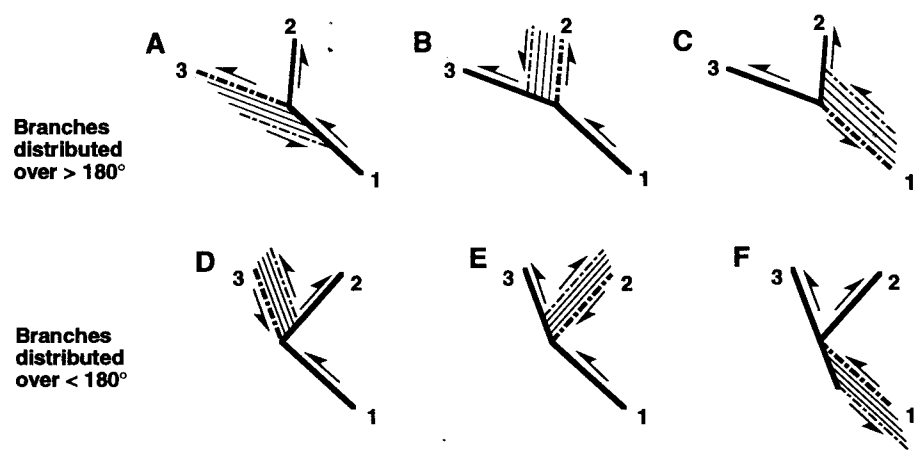

Fig. 2. Fault-fault-axial surface triple junctions that could accommodate shortening. Thick lines indicate active faults and active axial surfaces.

because we consider them most important to the low-temperature basement-involved structures of the upper crust (fig. 2A, B, D, and E).

The triple junction configuration of figure 2A was used to generate our prototypical model of figure 1. The triple junction configurations in figure 2A, B, D, and E are used to generate models in figure 3, A to D, which represent our four main classes of structures: *drape anticlines, fault-bend anticlines, fault-bend synclines,* and *wedge structures.* The models show the configuration of the basement without any cover strata. In figure 3, aa' is the active axial surface that emanates from a triple junction TJ. The stippled region S represents the material that has passed through an axial surface and is therefore deformed in response to fault slip.

In the case of drape anticlines and wedge structures (fig. 3A and D) the active axial surface travels with the hanging wall and decreases in length with increasing slip until the active axial surface is reduced to zero length and the triple junction ceases to operate (except for the special case of a wedge with the input fault parallel to the basement surface).

The triple junction is fixed in the footwall in the case of fault-bend anticlines and synclines (fig. 3B and C); therefore rock in the hanging wall sweeps through the active axial surface aa'. The active axial surface increases in length as slip on the main fault increases, except for the special case when the input fault is parallel to the basement surface in the model of figure 3C, wherein the axial surface length would be constant.

Different areas of the structure are progressively involved in the deformation in each of the four basic triple junction models. In figure 3A the undeformed triangle P is progressively reduced in size, whereas in the other three models the triangle is translated rigidly. In figure 3B and C shearing deformation occurs in rock of the hanging wall, and in figure 3D the footwall is the site of shear deformation. The shear strain indicated by the angle ψ in region S is a simple kinematic description of the strain that occurs in this region. This shear strain might be accomplished along a set of closely-spaced fractures parallel to the axial surfaces; however, the deformation in region S would probably be more complex in actual structures, as discussed below.

The relative displacements of fault blocks adjacent to triple junctions can be analyzed with vector triangles similar to the plate-tectonic vector triangles of McKenzie and Morgan (1969), as shown also by McCaig (1988). If the relative displacement of two blocks is known, then the displacement of the third can be determined by vector summation. Each of the models in figure 3 shows a vector triangle for that model. Our convention in constructing these vector triangles is to sum clockwise around the triple junction. Note that in figure 3A and B the hanging wall is uplifted at a greater rate than the triangle P, whereas in figure 3C and D the triangle is uplifted faster than the hanging wall.

Complex Geometries

Structures of greater complexity can be modelled by stringing together several of the four simple models of figure 3. For example Xiao and Suppe (1992) have accurately modelled large-scale folds in the

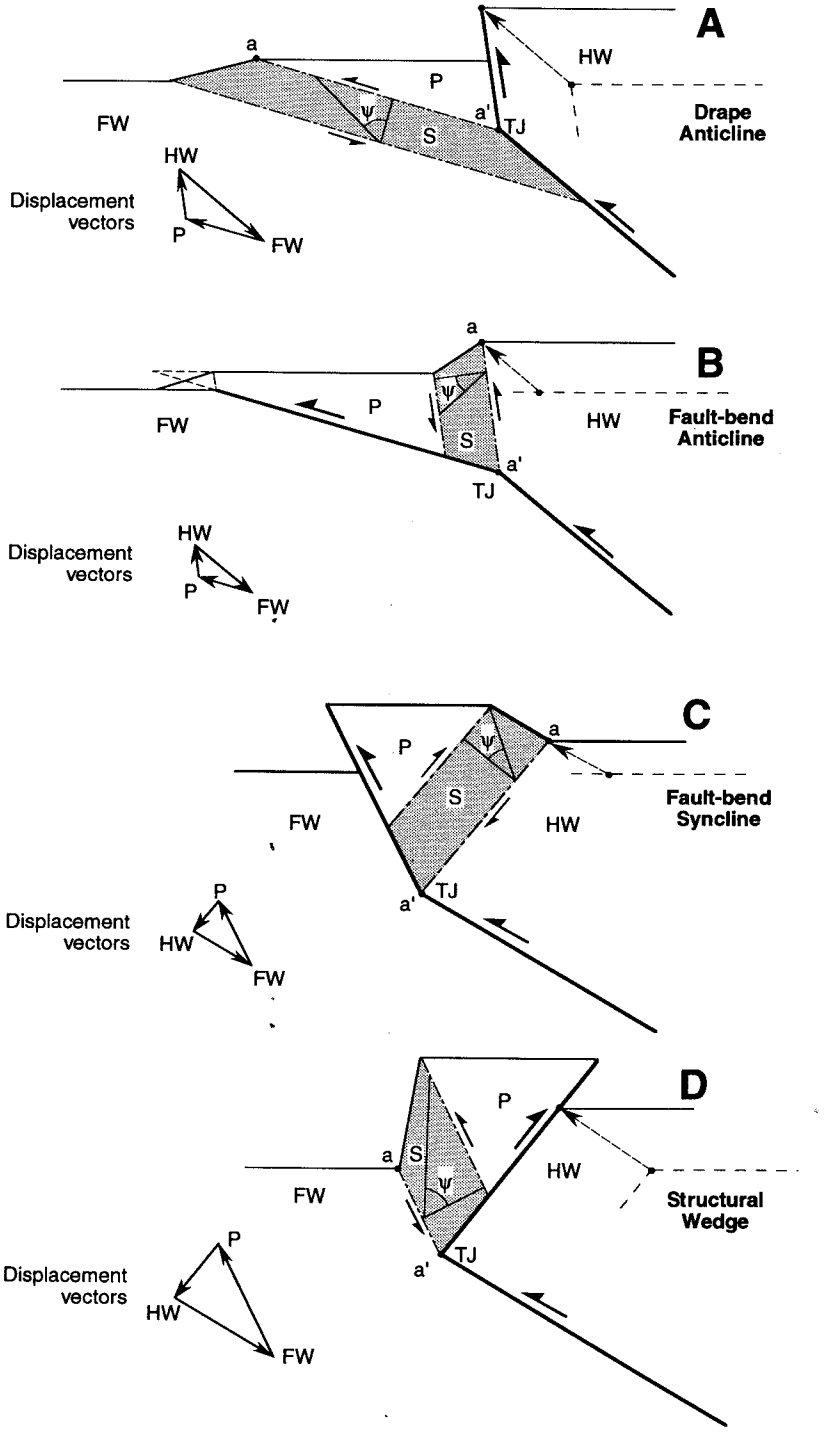

Fig. 3. Basement-involved structures that might form as a result of a fault-fault-axial surface triple junction where the lower branch is a fault. Vector diagrams show the displacement of each of the three basement blocks relative to the other blocks. *aa'* = active axial surface, ψ = angular simple shear strain, *FW* = footwall, *HW* = hanging wall, *S* = region that has been deformed in simple shear, *P* = rigid, wedge-shaped prism of basement.

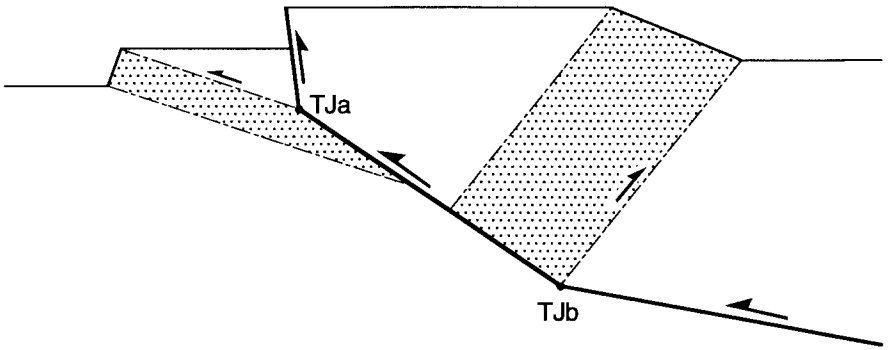

Fig. 4. Composite basement-involved structure involving two triple junctions. TJa produces a drape anticline, and TJb produces a fault-bend syncline.

hanging walls of continuously curved concave and convex normal faults by concatenating triple junctions. Figure 4 is a compressive model in which triple junction *TJa* is a drape anticline, and *TJb* is a fault-bend syncline. The triple junction on the left side of this figure could represent a typical basement-involved monocline—for example, an early phase of development of the southwest side of the Wind River Range—whereas *TJb* might be the panel of back dip—for example the northeast margin of the Wind River Range. (Note that this conceptual model is quite similar to the unscaled physical models of Chester, Logan, and Spang, 1991, especially their fig. 6C.)

Three-dimensional interaction of triple junctions may explain some long-standing problems of the changing transport direction of basement-involved structures. For example, the main fault on the east side of the Colorado Front Range—the Golden fault and its equivalents—dips westward (Dormorecki, ms), but a number of west-directed basement-involved structures form foothills east of the main range front, especially north of Boulder (Colton, 1978; Erslev, Rogers, and Harvey, 1988). This might result from a change in triple junction style from a drape anticline (fig. 3A) south of Boulder to a structural wedge (fig. 3D, as suggested by Erslev, Rogers, and Harvey, 1988) to the north. The west dip of the main input fault could remain the same, but its behavior near its upper termination is different. Likewise the transport direction of the Bighorn Mountains of Wyoming changes from west directed at their north end to east directed in the center of the range, then back to west directed at the south end. This could plausibly be a result of changing triple junction geometry in the upper crust with a single deep, main fault that persists along the length of the mountain block.

Although rather complicated structures can be modelled by concatenating triple junctions, higher-order junctions can also form. For example, figure 5 is a quadruple junction in which displacement on the main fault is partitioned onto two axial surfaces and an upper fault segment.

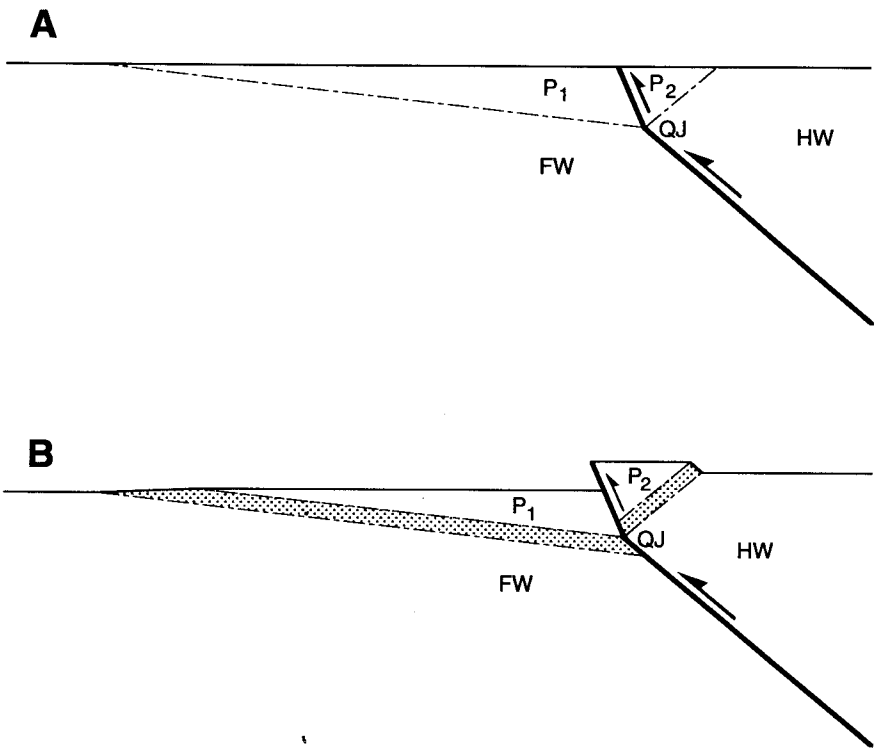

Fig. 5. Model of basement-involved structure resulting from fault-axial surface-fault-axial surface quadruple junction QJ.

Triple junctions can change character during development of a structure. The model in figure 6A initiates as a fault-bend anticline. The axial surface *bb'* at the narrow left end of triangle *P* (fig. 6B) behaves, in this example, according to conventional fault-bend fold theory (Suppe, 1983). If a fault forms along axial surface *aa'* in figure 6B—perhaps because some preexisting surface of weakness crosses the triple junction—an unstable fault-fault-fault triple junction forms instantaneously. A new axial surface must form, such as the one that nucleates from the gently-dipping fault (*ab*) and sweeps up through triangle *P* and the previously-deformed regions of basement (*aa"* in fig. 6C). This generates a steep fault in the basement: a drape fold would form in the cover over the basement corner.

In summary, a wide variety of triple-junction phenomena may be envisaged, even in two dimensions, which hold potential for explaining the diverse folding associated with faulting of basement in the upper crust. It should be noted that each of the models we have qualitatively discussed are quantitatively correct, using the quantitative theory presented below. Later we attempt to apply this general insight in a more specific way to relatively well-documented structures.

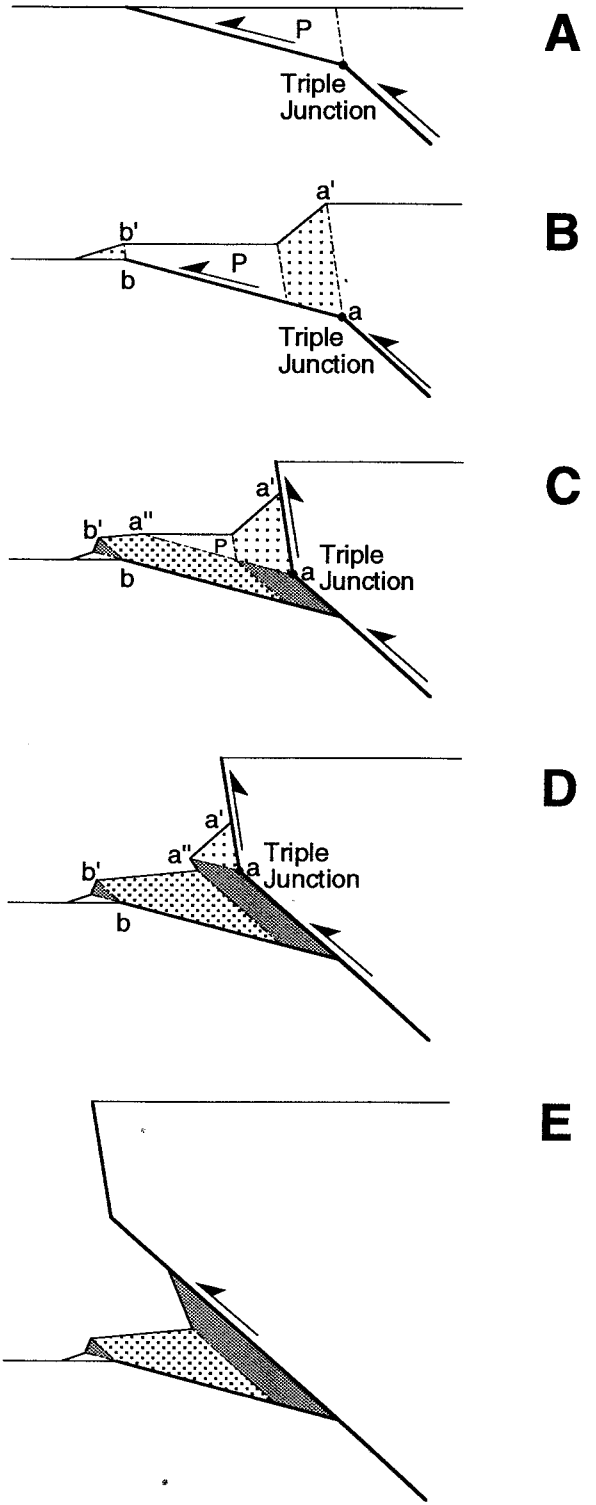

Fig. 6. Triple junction that changes character during the sequential development of a basement-involved structure. Axial surface *aa'* breaks through as a fault following step **B**, causing a new axial surface to form along the former fault *ab*. Axial surface *aa"* sweeps up through the prism *P* as well as through material that was previously deformed (steps **C** and **D**).

Deformation Mechanisms in Basement-Involved Structures and Orientations of Axial Surfaces

The conceptual basis for our triple-junction theory of basement-involved structures—beyond observational details of our specific case studies presented below—is simply the very old idea that some segments of faults propagating through the basement will lie along old faults and fabrics whereas other fault segments will be new in the Coulomb-fracture orientation. Alternatively, fault orientations may change direction due to local stress field perturbations, such as those that can occur in the vicinity of material interfaces, such as those that may result from changes in basement rock type, changes in material or frictional boundaries at the basement-cover contact, et cetera. Triple junctions will develop where active fault segments of different orientation join.

It is less obvious what determines the orientations of the axial surfaces. A wide variety of orientations is geometrically possible (for example, fig. 2). The actual orientation is determined by the deformation mechanisms. Many compressive structures in sedimentary sequences deform largely by slip on bedding-parallel faults in such a way that layer thickness is preserved; the axial surfaces take on orientations such that they bisect the interlimb angle. For this reason the theories of parallel fault-bend folding (Suppe, 1983) and fault-propagation folding (Suppe and Medwedeff, 1990) are based on conservation of layer thickness because they are designed for use in sedimentary sequences. In contrast, extensional folding commonly does not conserve layer thickness, because weak bedding planes are initially perpendicular to the maximum compression. Axial surfaces in extensional structures commonly take on the orientation of Coulomb fractures, dipping 65° to 70° antithetically in the case of concave fault bends and dipping 65° to 70° synthetically in the case of convex bends (Xiao and Suppe, 1992).

In the case of basement-involved structures, it is less clear a priori how axial surfaces will be oriented. That is to say, the geometric solution to the triple junction model has one greater degree of freedom than standard fault-bend fold theory involving bedding slip. Taking a clue from extensional structures, however, we might guess that the axial surfaces would be in the Coulomb orientation relative to the principal stresses, if slip is not activated on a preexisting planar structure.

Quantitative Relationships Between Fault Shape and Fold Shape

In this section equations are derived that describe the geometric development of the four basic triple junction models of figure 3. First, we derive a general equation that describes the change in angular position of a marker that experiences a simple shear strain. The results of this derivation are used to solve for the kinematic development of each of the four triple junction models of figure 3. The portions of these models that pass through an active axial surface (stippled in fig. 3) can be treated kinematically as having experienced a simple shear through an angle ψ.

Consider the kinematics of deformation in the model of figure 7. The displacement vector of the hanging wall block aa' is parallel to the

main fault, and the vector *aa"* shows how material in the triangle above the active axial surface (*b'c'*) is translated. A line that was orthogonal to the axial surfaces prior to deformation, *cd*, is sheared through the angle ψ to *c'd* (note *cc'* = *aa"* in length and direction). So, the angular simple shear experienced by material between the axial surfaces is:

$$\tan \psi = \frac{cc'}{cd} \tag{1}$$

where ψ is measured from a line perpendicular to the direction of shear displacement (the axial surfaces), and counterclockwise angles are positive.

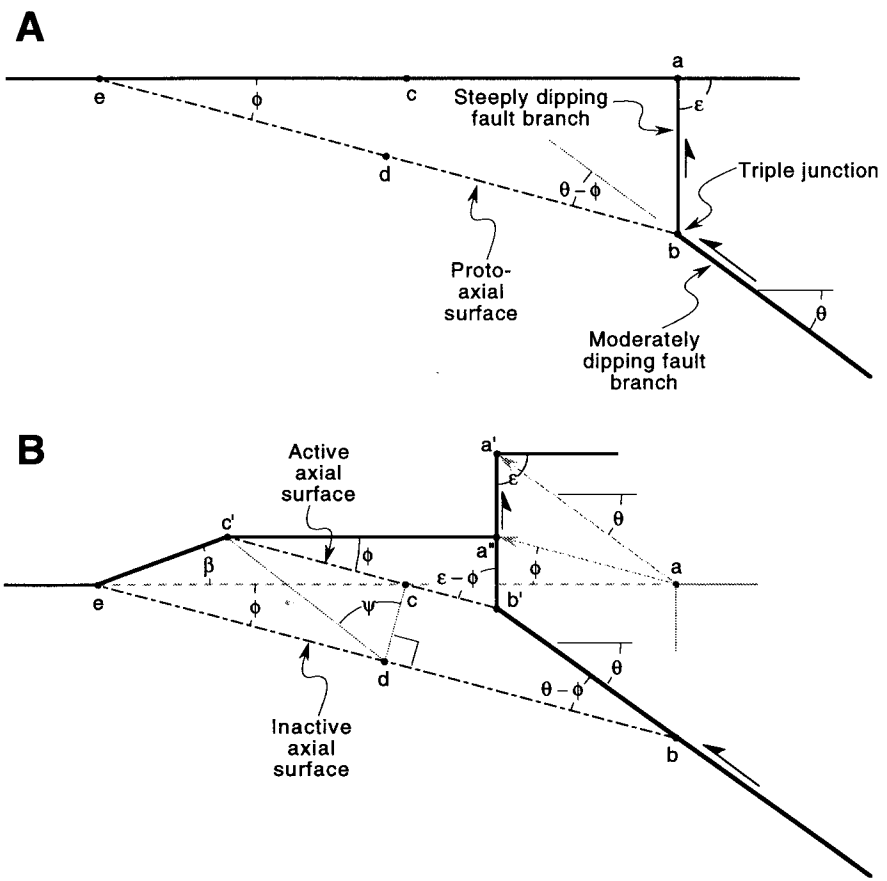

Fig. 7. Drape anticline triple junction model showing its fundamental related angles before fault displacement (**A**) and after a finite displacement (**B**). The triple junction is located at *b'*. The material that lay originally at point c in the model prior to deformation has been translated to *c'*, so the line *cd* that is orthogonal to the axial surfaces is sheared by an angular simple shear of ψ to *c'd* during deformation.

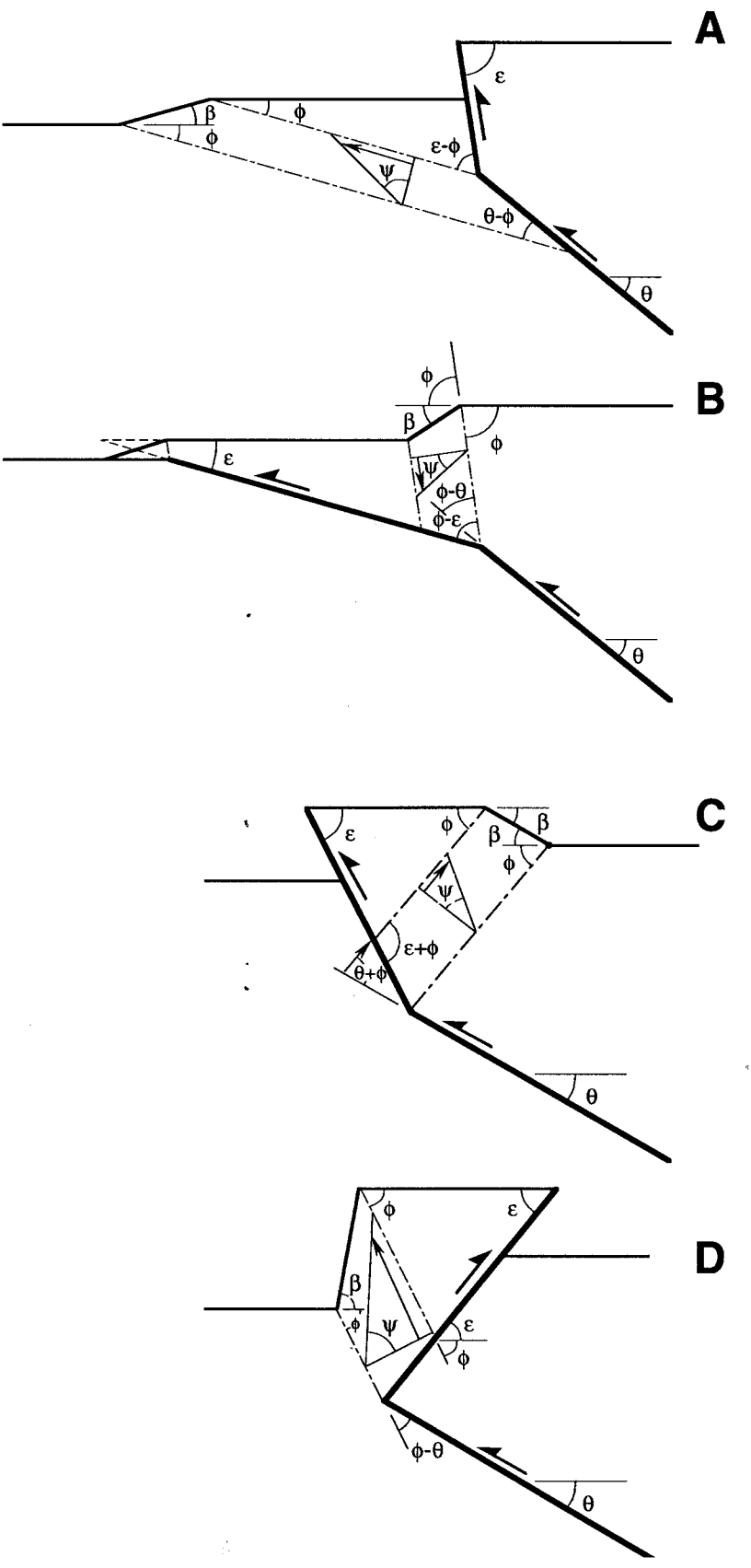
A
ε
β
ϕ
ϕ
ε-ϕ
ψ
θ-ϕ
θ
B
ϕ
β
ϕ
ε
ψ
ψ
ϕ-θ
ϕ-ε
θ
C
ε
ϕ
β
β
ϕ
ψ
ε+ϕ
θ+ϕ
θ
D
ϕ
ε
β
ϕ
ψ
ε
ϕ
ϕ-θ
θ

We will define model angular relationships relative to the original basement surface (shown horizontal in fig. 7). The line *ce*, which lies along the horizontal basement surface prior to deformation, makes an angle ϕ with respect to the inactive axial surface *be*. During deformation, point *c* is displaced to *c'* parallel to the active axial surface. The deformed basement surface has a dip β relative to its original attitude, and *c'e* takes an angle $\phi + \beta$ relative to the inactive axial surface. The displacement *cc'* can be expressed as:

$$cc' = cd \cot \phi + cd \cot (180° - (\beta + \phi))$$

where angles are expressed in degrees. Dividing by *cd* and combining with eq 1 we obtain:

$$\frac{cc'}{cd} = \tan \psi = \cot \phi - \cot (\beta + \phi) \tag{2}$$

which is equivalent to eq 2.3 of Ramsay and Huber (1987) except for a difference in sign convention. This equation is used to solve for angular relations of models generated with different triple junction geometries. In figure 7 (also fig. 8A) the other angles important to this model, θ (dip of the main fault branch) and ϵ (dip of the steep fault branch) are kinematically related to simple shear between the axial surfaces by:

$$\tan \psi = \cot (\theta - \phi) - \cot (\epsilon - \phi) \tag{3}$$

All angles are specified with respect to the regional dip, which is horizontal in the models of figures 7 and 8. The reference direction from which angles are measured is important; note that both ϵ and β can be greater than 90°. Eqs 2 and 3 are equated and solved to find the fundamental angular relations for this triple junction geometry
(*case fig. 8A*)

$$\theta = \tan^{-1} \left[\frac{1}{\cot \phi - \cot (\beta + \phi) + \cot (\epsilon - \phi)} \right] + \phi \tag{4}$$

The angular relations of the other models of figure 8 are solved similarly. For the models of figure 8B and D

$$\tan \psi = \cot \phi - \cot (\beta + \phi) \tag{5}$$

and

$$\tan \psi = \cot (\phi - \theta) - \cot (\phi - \epsilon) \tag{6}$$

are equated to find

(*cases fig. 8B, D*)

$$\theta = \phi - \tan^{-1} \left[\frac{1}{\cot \phi - \cot (\beta + \phi) + \cot (\phi - \epsilon)} \right] \tag{7}$$

Fig. 8. Basement-involved structure models showing angles that are used in eqs (3) to (13).

The angular relations in model 8C are based on

$$\tan \psi = \cot (\epsilon + \phi) - \cot (\theta + \phi) \tag{8}$$

and

$$\tan \psi = \cot (\beta + \phi) - \cot \phi \tag{9}$$

which equate to

(*case fig. 8C*)

$$\theta = \tan^{-1} \left[\frac{1}{\cot \phi - \cot (\beta + \phi) + \cot (\phi + \epsilon)} \right] - \phi \tag{10}$$

The solid curves in figure 9 show, for $\epsilon = 90°$, the relationship between θ and ϕ at values of $\beta = 1°, 2°, 5°, 10°, 20°$ and increments of 20° up to 160° for a drape anticline triple junction (fig. 8A). The dashed curves show the angular simple shear ψ for the same increments of β.

Figure 10 shows the angular relations between lower fault dip θ and fault bend ϕ for values of upper fault dip ϵ in 20° increments from $\epsilon = 40°$ to $\epsilon = 140°$ and fold dip β from 10° to 160°, for the drape anticline triple junction (case fig. 8A). These plots bracket the range of solutions for the majority of drape anticline basement-involved structures. Notice that the scales of the θ and ϕ axes are different in the different plots of figure 10; scales range across the entire permissible range for each specific geometry. In fact the graphs of figure 10 are simply slices through a three-dimensional volume with three orthogonal axes, ϕ, θ, and ϵ, within which constant values of β are described by curved surfaces. Similar plots can be made for the other triple-junction types of figure 8 using eqs 7 and 10.

The plots of figure 10 may be useful for finding approximately acceptable model solutions when interpreting basement-involved structures. When using these models to interpret a structure it is necessary to know three independent angles to solve uniquely for the fourth. From a practical standpoint, given commonly incomplete data, these plots and equations are more useful as a component of a forward kinematic model (Mount, Suppe, and Hook, 1990) than for interpreting hidden structure based on partial data.

The appropriateness of these models to actual structures is explored in the following section using observations of the geometry of six structures in the eastern Rocky Mountains.

TESTING THE MODEL: *CASE STUDIES OF THE GEOMETRY AND KINEMATIC DEVELOPMENT OF BASEMENT-INVOLVED STRUCTURES*

The triple-junction structural models described above were inspired by observation of a number of well constrained basement-involved structures, six of which are discussed below and are located on figure 11. We present quantitative retrodeformable cross sections of the first three

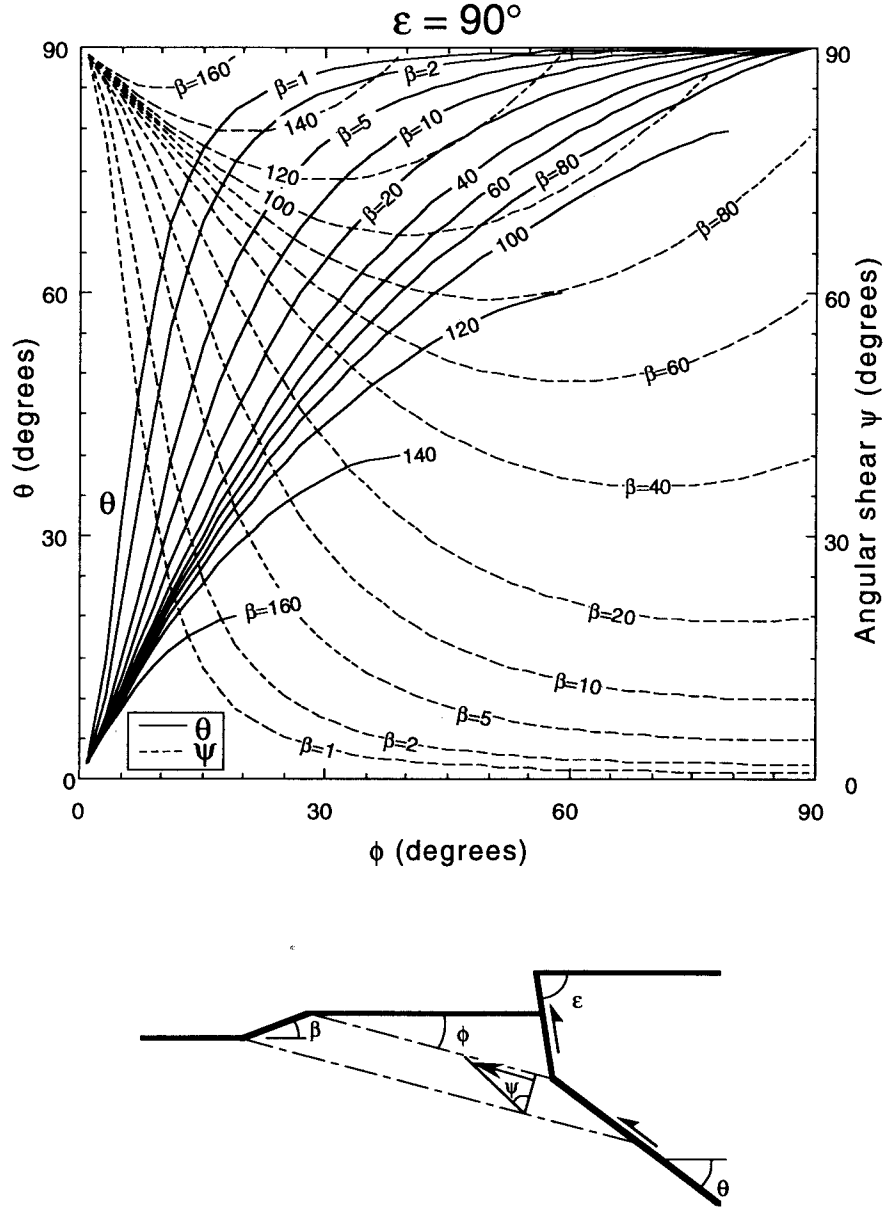

Fig. 9. Relationship of θ versus ϕ (solid curves) and ψ versus ϕ (dashed curves) for ε = 90° and for values of β across a range from 1° to 160° for drape anticline triple junctions.

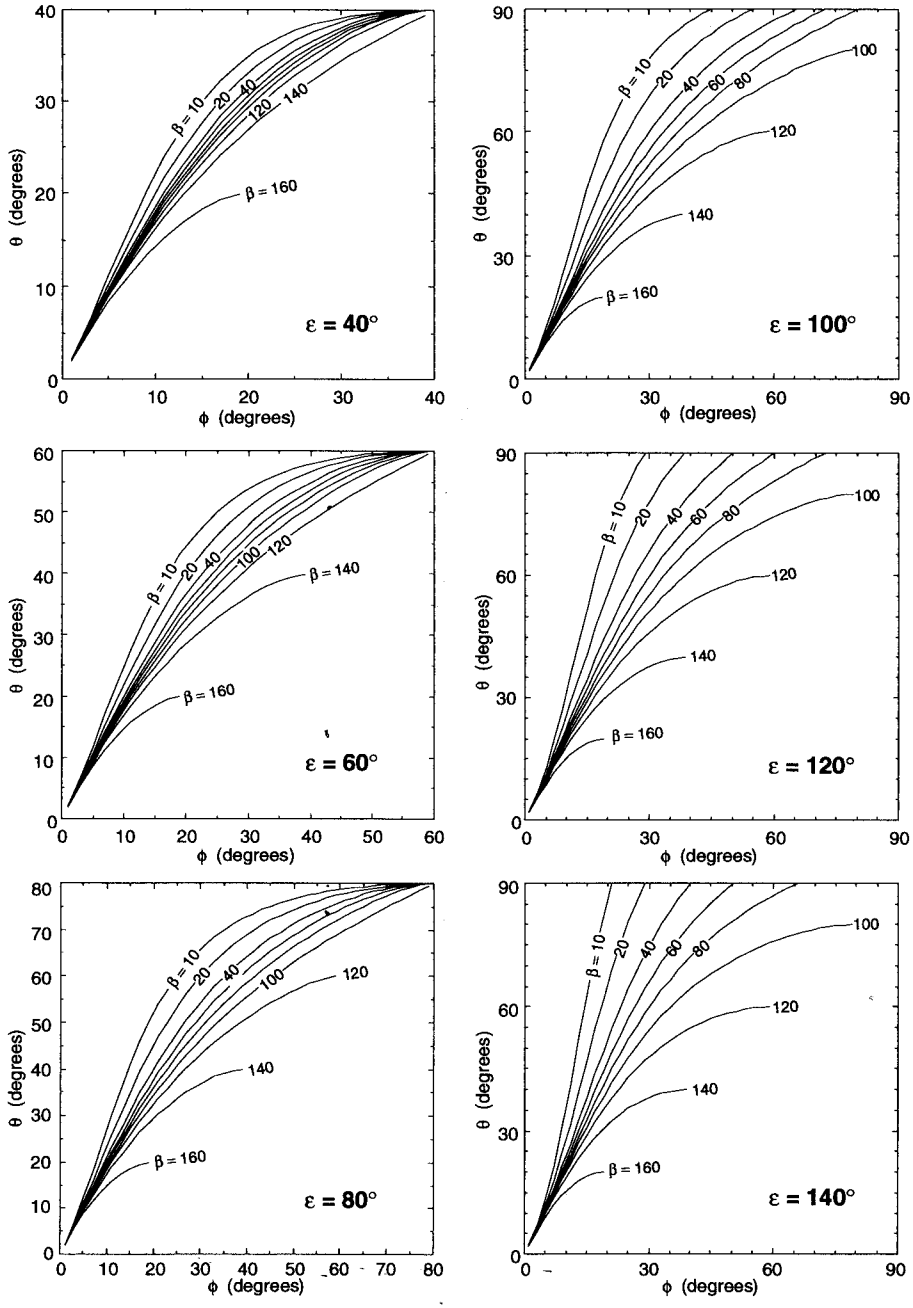

Fig. 10. Relationship of θ versus ϕ for values of β at 10°, 20°, and at 20° increments to 160°, for ε = 40°, 60°, . . . , 140°, for drape anticline triple junctions.

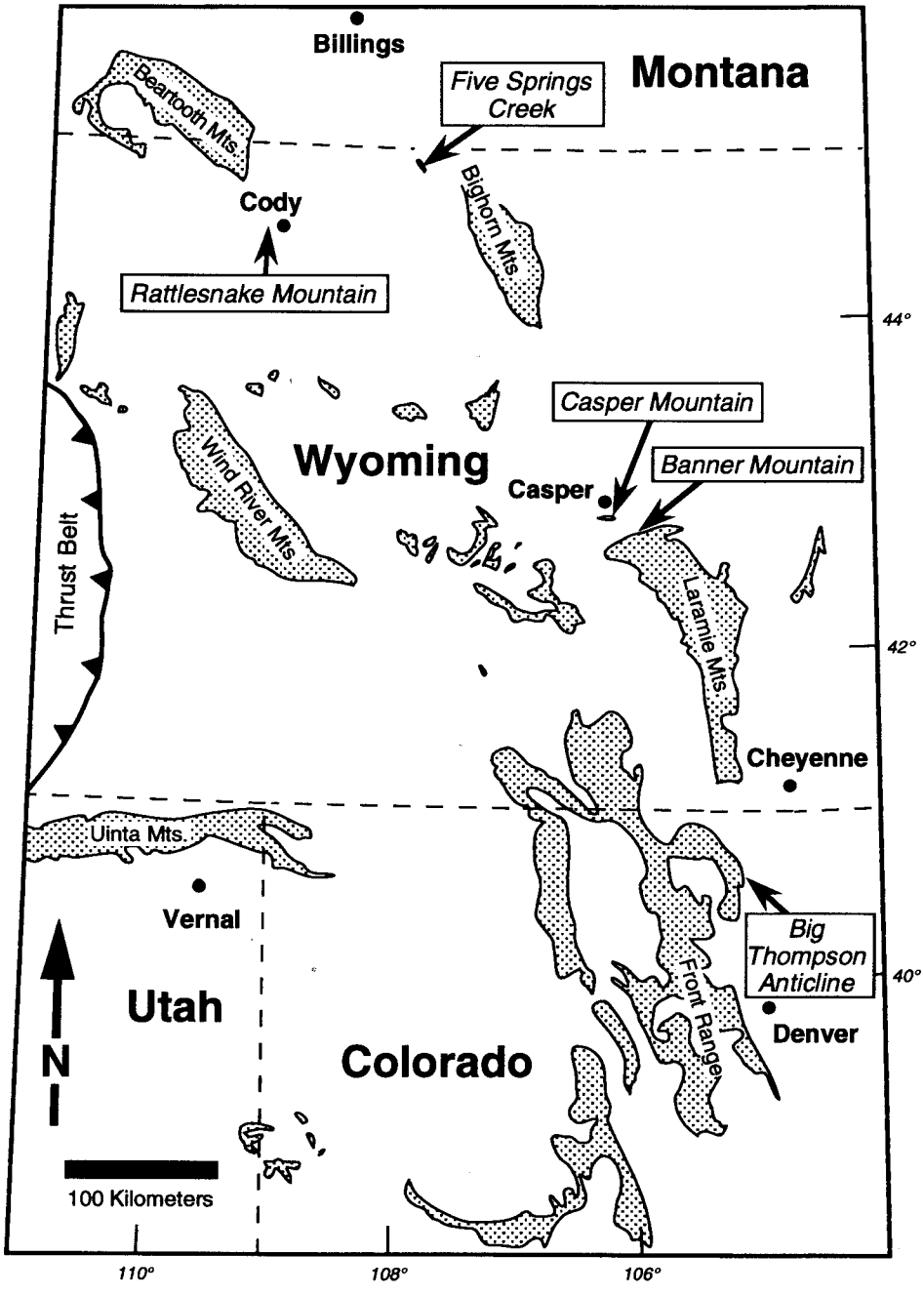

Fig. 11. Index map of the eastern Rocky Mountains showing location of the sites discussed (after Stearns, 1978). Stippled areas show surface exposure of basement rock.

structures, whereas the last three structures are compared more qualitatively with the predictions of the triple-junction models. A brief summary is given for each structure followed by the detailed description and analysis in a smaller typeface. Structural data were collected at closely spaced intervals along cross-sectional traverses, with several traverses for each structure. Gravity data were collected for three structures.

Big Thompson Anticline

Summary.—Big Thompson anticline is one of a set of south-plunging, west vergent basement-cored anticlines in the foothills Front Range of Colorado, three of which are shown in figure 12. Viewing these structures down plunge we see that the faults die out up dip within the steep, even overturned, west limbs of these rather angular folds. A profile cross section of Big Thompson anticline (fig. 13), which displays projected dip data, shows a strongly angular, straight-limbed fold geometry and a structural disharmony between basement and cover. This disharmony is all the more profound because outcrop studies show that the basement has not been appreciably folded (Erslev, Rogers, and Harvey, 1988; Narr, 1993). The deep fault geometry has been constrained by a gravity survey (fig. 14), the profile projection, and outcrop measurements. A retrodeformable kinematic model (fig. 13) involving a fault-fault-fold triple junction in the basement similar to our prototypical models (figs. 1 and 3A), a detachment between basement and cover, and wedging within the cover accounts quantitatively for the key observational constraints—in agreement with our thesis. It is important to note in this solution that the basement has not been folded in the hanging wall of the thrust.

Surface structural geometry.—Big Thompson anticline (also called Milner Mountain or Loveland anticline) is a south-southeast plunging, west-vergent fold in the eastern foothills of the Front Range, 5 km west of Loveland, Colorado (figs. 11, 12). The geometry of this structure is constrained by field data, a local gravity survey, and regional well data.

Viewing the geologic map (fig. 12) down plunge we see that the Milner Mountain fault, which juxtaposes basement against Pierre Formation on the west side of the anticline, terminates down plunge near the synclinal axial trace, which is similar to fault terminations in fault-propagation folds (Suppe and Medwedeff, 1990). Near this termination, strata in the steep limb have been tectonically thinned and overturned.

It is also seen that the shape of the top of basement is conformable with the fold shape higher in the cover. In this area, strata on the east flank of the anticline dip 15° to 25°, whereas strata on the west flank are steep to overturned. Based on these observations we might guess that the basement is strongly folded; however, it is clear from measurements of foliation attitude taken along four traverses across the basement in the southern plunge of the structure that there has been no appreciable rotation of the basement during the Laramide orogeny (Narr, 1993). Erslev, Rogers, and Harvey (1988) measured foliation along several traverses north of the junction of the Fletcher Hill and Milner Mountain faults, and they also conclude that the basement in that portion of the anticline has not been significantly rotated. The basement rock is Precambrian schist with steeply-dipping, northwest-striking foliation; thus it may be in mechanically inappropriate orientation for folding. The dashed fault between the Fountain Formation and basement on the west side of the

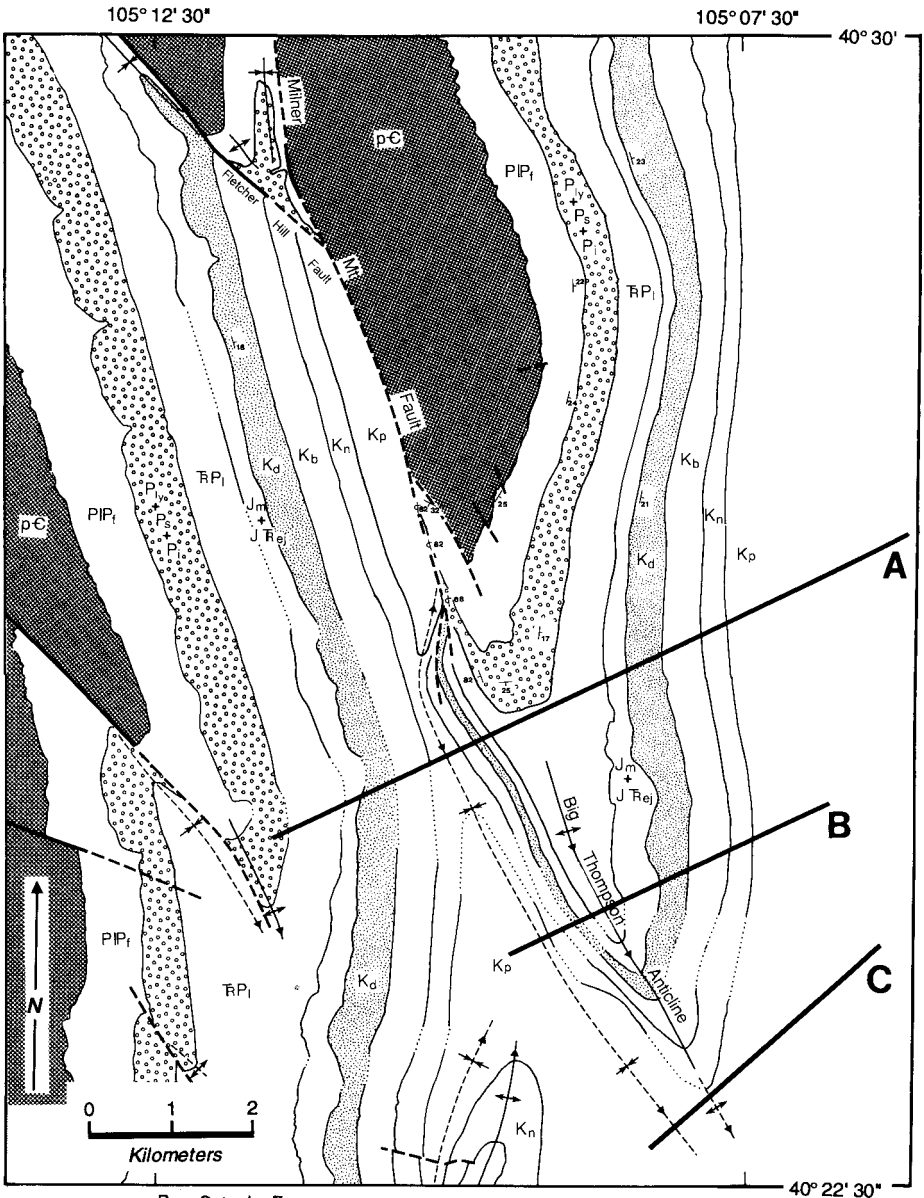

Fig. 12. Geologic map of Big Thompson anticline. A, B, and C show the strike of profile planes, as well as southern limits of cylindrical segments of the structure, used to construct down-plunge projection. Based on Braddock and others (1970) and our field work.

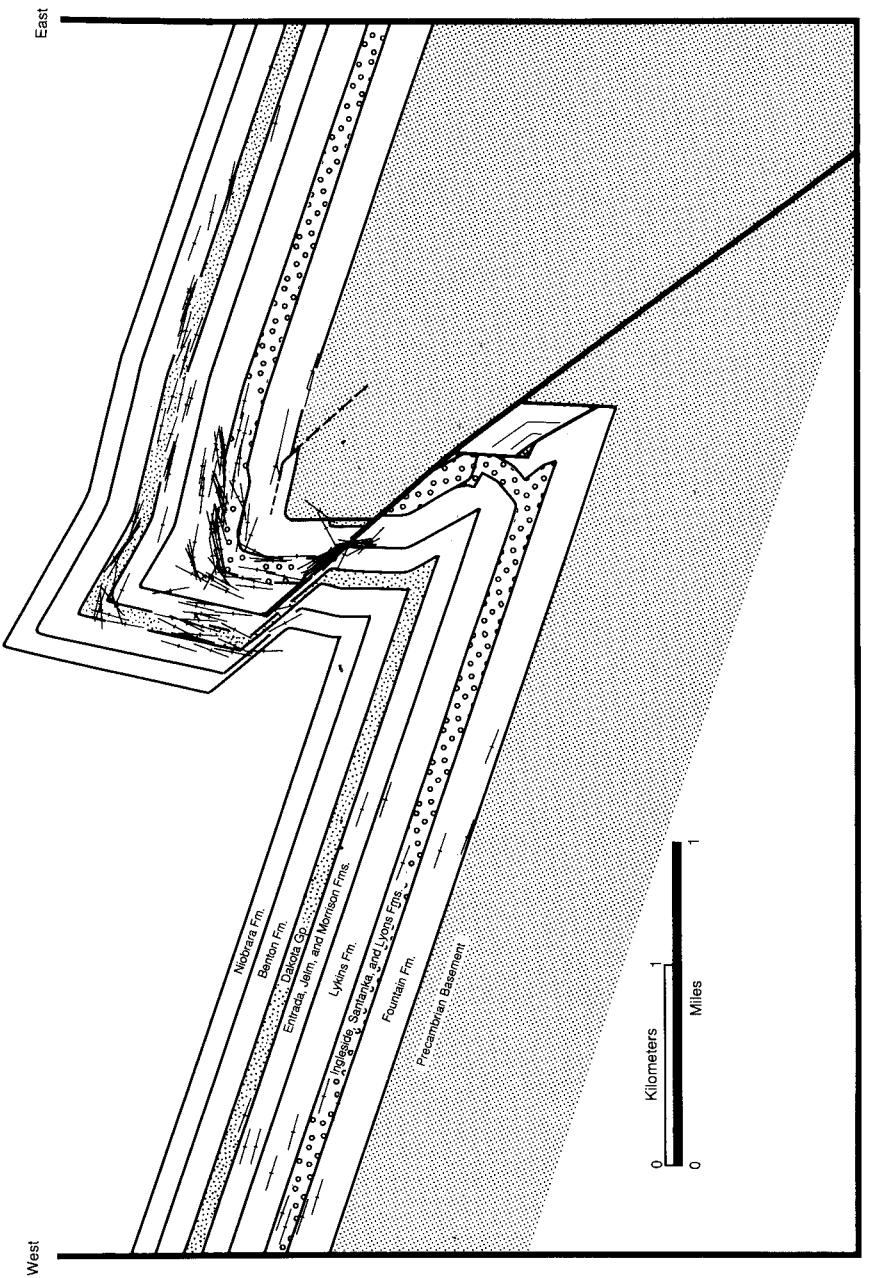

Fig. 13. Geologic cross section of Big Thompson anticline, based on composite down-plunge projection (see text for discussion of construction method). Barbed bars indicate projected dip of bedding.

anticline is not on the map by Braddock and others (1970), but a fault must be present here if the basement is not rotated (compare fig. 13).

Construction of profile section.—Big Thompson anticline is not cylindrical, which is apparent in the expanded width of the Lykins Formation, which contains bedded gypsum, and in the change in plunge of the syncline near the fault termination. The non-cylindrical nature is also evident from the change in stratigraphic throw on the Milner Mountain fault—in the north the basement has slipped beyond the base of the Pierre Formation, but in the south it does not cut the Pierre.

The non-cylindricity has a significant effect on projection of structural data onto a profile plane for construction of a cross section (fig. 13). The fold was divided longitudinally into three principal domains based on inspection of the structural data from the entire fold (data were collected in relatively high density over the entire structure). Domain *A* extends for about 4 km north of line *A* in figure 12, domain *B* is between lines *A* and *B*, and domain *C* is between lines *B* and *C*. Apparent structural attitudes and formation contacts within each domain were projected onto profile planes perpendicular to best fitting fold axis of the domain. The profile planes were then stacked vertically to construct the profile section (fig. 13).

The profile section (fig. 13) shows that Big Thompson anticline is an angular monocline with an interlimb angle of about 80° to 90°. Bedding in the hanging wall and footwall are parallel to the same regional dip. The Lykins Formation is thickened in the anticlinal hinge, although much of the apparent thickening in map view (fig. 12) is due to the relatively gentle plunge through this region. The Lykins Formation consists of fine-grained clastics, thinly-bedded limestone, and bedded gypsum. An abandoned gypsum quarry in the thickened hinge provides excellent exposures that show considerable evidence of layer-parallel shortening including trains of buckle folds, some of which are isoclinal, with wavelengths ranging from centimeters to meters. Their axes parallel the best fit axis

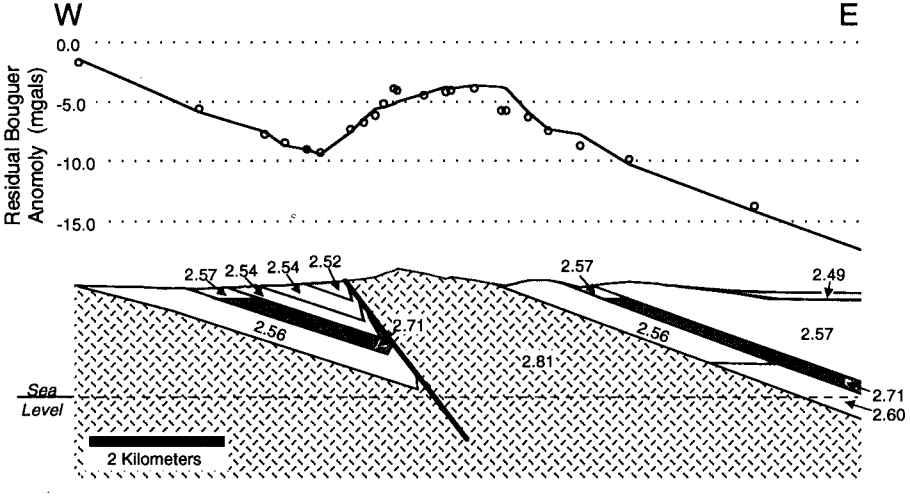

Fig. 14. Residual Bouguer anomaly of Big Thompson anticline, along a vertical profile plane orthogonal to axial trace and approx 1.3 km south of the junction of the Milner Mountain and Fletcher Hill faults. Open circles are based on measured data; solid curve is computed based on the model beneath the graph. Model densities are labeled in g/cm^3.

determined for this portion of Big Thompson anticline, which suggests that the minor folds and the main anticline formed during the same structural episode.

Dip of the fault.—The dip of the Milner Mountain fault is constrained in several ways. Erslev, Rogers, and Harvey (1988) interpret the Milner Mountain fault to dip 60° east based on field observations of a fault plane near the Fletcher Hill fault. The down-plunge projection of the hanging wall cutoffs of the Fountain, Lyons, and Lykins Formation suggests the fault dips 49° east, with a similar dip for the overturned bedding in both the hanging-wall and footwall (fig. 13).

Gravity data further constrain the dip of the fault, based on the contrast in density between the basement and cover. Narr (ms) did a local gravity survey of the area for this purpose, including a close-spaced profile across the central portion where the basement displacement is a maximum. Open circles in figure 14 show the residual total Bouguer anomaly after removal of a linear regional gradient. The solid curve shows the computed residual gravity of the model. The model that best approximates the observed gravity data has a fault dip of 52° east (±10°).

The three independent estimates of the fault dip are in close agreement—60° from the field observations of a fault plane by Erslev, Rogers, and Harvey (1988), 49° from projection of map data onto a profile plane, and 52° from gravity modeling.

Kinematic model–generalities.—To a non-specialist the construction of retrodeformable forward models such as figures 15 and 18 is imbued with mystery. The approach used is essentially that mapped out by Mount, Suppe, and Hook (1990). Briefly, (1) the data are assembled in a cross section presumed to contain the displacement vectors; (2) a provisional cross-sectional hypothesis is constructed; (3) a retrodeformable forward model of the hypothesis is constructed, using for example our quantitative triple-junction theory, beginning with the undeformed state; (4) the final stage of the model is compared with the data of step 1, adjustments are made in the cross section of step 2, then we return to step 3 and construct a revised forward model; (5) we iteratively continue the process until we arrive at both a cross section and model that are satisfactory for our purposes, or until we collapse in exhaustion because we have not guessed the essence of the structure from the available data.

Kinematic model.—Figure 15 illustrates the kinematic development of Big Thompson anticline, viewed in the same plane as figure 13. The structure initiates as a drape anticline with $\theta = 35°$, $\phi = 21.5°$, $\epsilon = 71°$, and $\beta = 106°$ (this uses a 53° dip for the Milner Mountain fault and 18° for the regional dip). The vertical edges on the model are pin lines of equal bed length.

In figure 15B the active axial surface has just reached the top of the deformed triangle of material in the basement. The basement in the hanging wall is not rotated. The cover is draped over the basement edge. Below the Lykins Formation a contractional fault has formed in the steep limb near the syncline. This displacement is transmitted by simple shear across the Lykins to form the disharmonic lift-off in the crest of the anticline. The dashed line *F* in the steep limb is the site where an extensional fault will develop as deformation progresses beyond this stage. The parallel lines in the Fountain Formation near the syncline are markers to show how this part of the structure develops.

In figure 15C basement of the hanging wall has begun to penetrate the cover. Extension occurs low in the cover sequence by rounding-off the hinge of the anticline (which also modifies the shape of the anticline to the uppermost layer in the model) and by slip along the fault labeled *F* in 15B (which is folded and lies along the west edge of the overturned Fountain strata in the footwall in 15C). A bed length imbalance of a maximum of 100 m develops above the Lykins Formation, as illustrated by the bent pin on the left side on this figure. These strata are eroded off a few kilometers west of Big Thompson anticline, so evidence of this displacement is not seen.

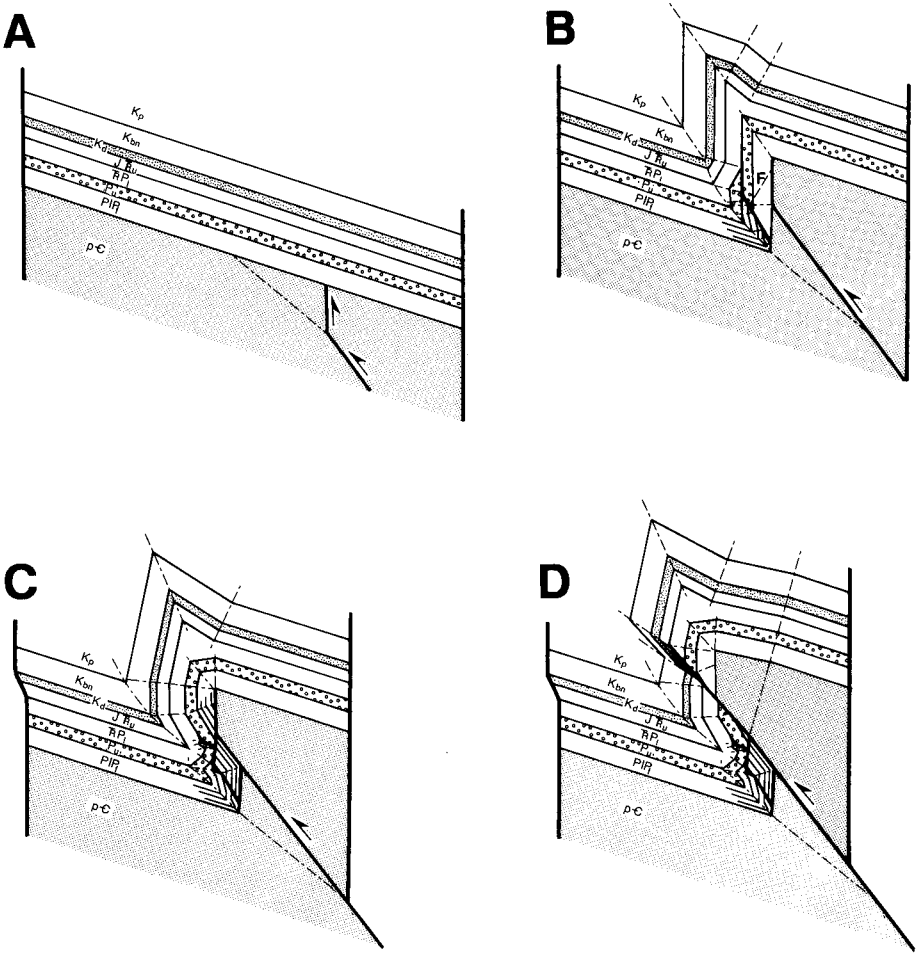

Fig. 15. Cross sections showing the kinematic sequence of development of Big Thompson anticline, in same profile view as figure 13.

In the final stage of the kinematic model (fig. 15D) a minor fault-bend fold affecting hanging wall basement forms above overturned Fountain strata of the syncline. The main fault breaks through the cover up to the top of the Lykins Formation. Stratigraphically above the Lykins, strata are stretched, thinned, and overturned. In effect, the Milner Mountain fault is discrete below the level of the top of the Lykins but becomes a wider fault zone at shallower levels.

Willow Creek Anticline

Summary.—Willow Creek anticline is unusually well constrained by surface and well data (figs. 16 and 17). Well data suggest that the

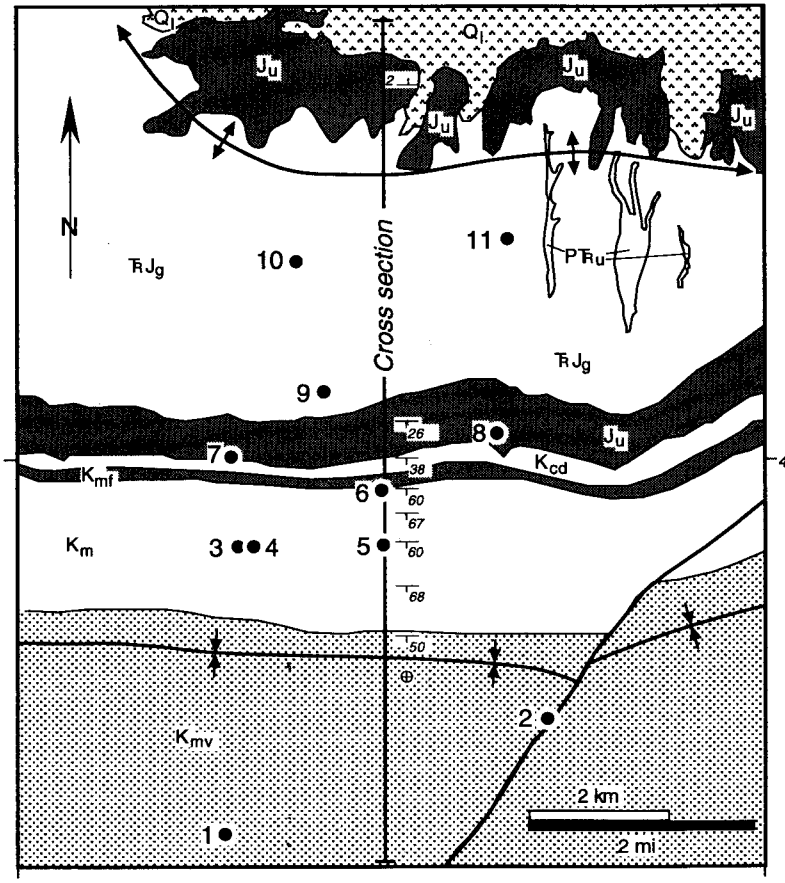

Map Formations

Q	Quaternary Landslide
K_{mv}	Mesaverde Gp.
K_m	Mancos Fm.
K_{mf}	Mowry and Frontier Fms.
K_{cd}	Cedar Mt. and Dakota Fms.
Ju	Jurassic Undivided (Carmel, Entrada, Stump, and Morrison Fms.)
TRJg	Glen Canyon Fm.
PTRu	Permian-Triassic Undivided (Chinle, Moenkopi, and Park City Fms)

Well Key

1. Petro-Lewis Calvin Fed # 1
2. McLaughlin 1-24 Govt
3. Brooks #1 State 16
4. Triton O&G Co. 1-16 State
5. Pure #1 Govt
6. O'Neill Federal R #1
7. Avance O&G Co. Federal #1
8. Mobil Oil Co. North Rangely #1
9. Tenneco #1-A Hicks-Govt
10. Pan American Petrol. Anderman #1
11. E. American Tully #1

Fig. 16. Geologic map of Willow Creek anticline area, showing representative bedding attitudes and well locations. Map is based on Cullins (1969), Rowley and Hansen (1979), and our mapping.

basement is not strongly folded, in contrast with the cover. The steep and overturned strata of the cover appear to be conformable to faults in the basement, similar to Big Thompson anticline (fig. 13) and to our drape anticline prototypical model (fig. 1). In particular the basement-cover contact in the steep southern limb of the anticline appears to be a fault—similar to the steep, drape-induced detachment of our model—and not a folded unconformity. The main Willow Creek thrust appears to be a reactivated, Precambrian normal fault. This thrust disappears updip at the synclinal axial surface in the cover (fig. 17), with displacement probably wedging back along a decollement within the Mancos Formation. The anticline has an overall rounded shape but is in fact composed of panels of constant dip separated by angular hinges. The final shape is a result of both the initiation of this anticline as a drape fold and subsequent fault-bend folding as the hanging wall moved forward over flattening-upward fault bends. The retrodeformable kinematic model (fig. 18) closely mimics the actual data, in support of our model of drape anticline, triple-junction folding.

Structural constraints.—Willow Creek anticline is an east-west trending, south-verging monocline in northwest Colorado (fig. 16) whose structure is unusually well constrained by surface geology, oil exploration wells, and seismic data. It has been discussed by Berg (1962), Gries (1983), and Powers (1986).

Figure 16 is a geologic map of the Willow Creek area based on Cullins (1969) and Rowley and Hansen (1979). Representative bedding attitudes are shown along the line of cross section (fig. 17), which in the Mancos Shale were obtained by digging shallow pits through the weathered surface (Narr, ms). Dips were not used from the Glen Canyon Formation because of ubiquitous high-angle cross bedding. At surface exposures and in wells the strata form panels of approximately constant dip, with changes in dip restricted to narrow hinge zones. For example a dip change of 65° occurs across the synclinal axial surface in the Mesaverde Formation, and most of this dip change occurs across a hinge zone a few tens of meters wide. Likewise the anticlinal dip change that occurs at the surface between wells 6 and 7 occurs across a very narrow region. The dip changes seen in the dipmeter log of well 8 are similarly abrupt. These abrupt dip changes show that the rounded structural form depicted by Berg (1962), Cullins (1969), Gries (1983), and Powers (1986) is in fact not continuously curved, which is a key structural observation to be explained.

Subsurface dip measurements were made from core in wells 5 and 9. Well 8 was logged by a modern 4-arm dipmeter that was used to compute both well deviation and bedding dip. The deviations of all wells other than 8 are interpreted, based on fitting their formation thicknesses and relative attitude data with surface geology and well 8 (Narr, ms).

Notwithstanding uncertainties about well deviation and additional uncertainties caused by the projection of data into the plane of cross section, the position of the Willow Creek fault is tightly constrained. Precise fault intersection depths are determined in wells 6 and 9. Wells 4, 7, and 8 intersect the fault in intervals that were not logged. Wells 3 and 5 correlate in the lower portion of the Mancos, but above 1250 m depth their correlation is not clear, probably due to steep dip. These wells must penetrate the fault above this depth.

In our interpretation the fault cuts well 5 just above the depth of the lower core, at about 1220 m depth, placing near-vertical Frontier-Mowry strata above the Mancos Formation. Just south of well 3 the fault flattens onto a decollement, then reverses its transport direction to form a structural wedge and send fault displacement up the steep

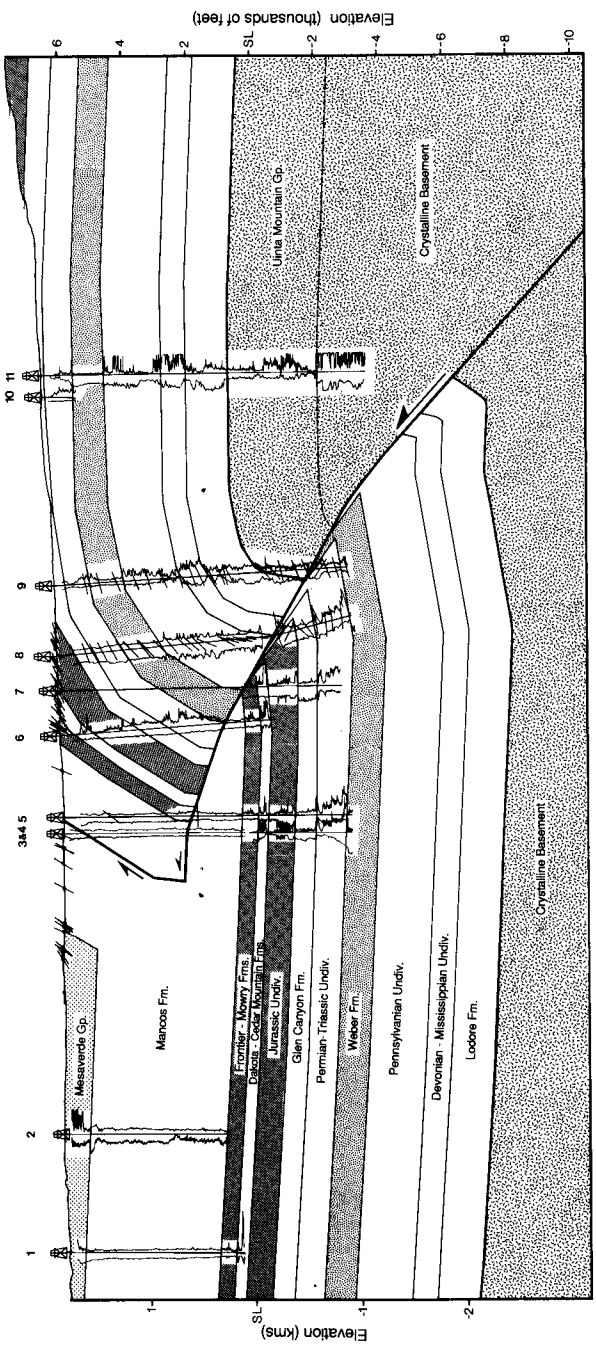

Fig. 17. Geologic cross section of Willow Creek anticline. Section location and well key are on figure 16. Short bars along topographic profile and in wells 5, 8, and 9 show bedding dip.

limb along a decollement in the Mancos Formation. The surface location of the Willow Creek fault is unknown as the Mancos Formation is poorly-exposed virtually everywhere.

Another feature of this and many basement-involved structures is a relatively narrow zone of overturned, tectonically thinned strata beneath the fault (fault sliver of Gries, 1983) in wells 8 and 9. The dip of the overturned beds is close to the inferred dip of the Willow Creek fault, similar to what was observed below the Milner Mountain fault of the Big Thompson anticline (fig. 13) and similar to our simple prototypical model of basement-cover interactions (fig. 1).

Basement is not exposed at the surface but is penetrated by wells 9 and 11. It consists of Proterozoic Uinta Mountain Group which is massive, coarse quartzose and arkosic sandstone and conglomerate with minor interbedded shale and argillite (Rowley and others, 1985) which overlies true crystalline basement. In spite of its bedded character, the Uinta Mountain Group behaved similar to the crystalline basement at other sites studied. Dipmeter data through the Precambrian in well 9 show consistent gentle to moderate south dips from beneath its upper contact with the Cambrian Lodore Formation through to the underlying fault. These data show that basement is not folded to the steep attitude of the basement-cover contact, in contrast with Powers (1986). If the basement were strongly folded in this position some evidence of steep strata would be evident on the dipmeter and electric logs of well 9 (compare for instance the dipmeter data in the steep beds above the fault in well 8). Thus the steep southern contact of the basement must be a fault, similar to the fault at Big Thompson anticline (fig. 13) and to our simple prototypical model of basement-cover interactions (fig. 1).

In contrast with the basement, dip data in the lower part of the Cambrian Lodore Formation in well 9 are erratic (not shown in fig. 17). However, the resistivity log in this interval correlates to well 11 without difficulty. These observations suggest minor folding or faulting, which can strongly affect dipmeter measurements, but an overall intact lower Lodore Formation. The disrupted dips are likely an effect of drape folding of the cover over the uplifted basement corner (compare fig. 1).

Kinematic model.—The kinematic development of Willow Creek anticline is illustrated with a forward model in figure 18. The dashed lines at either end of the sections, labeled P and P', are pin lines that record equal bed length as the anticline develops. The positions of the hanging wall cutoffs of the Willow Creek thrust are tightly constrained by wells in the steep limb, therefore we measured the lengths of beds in the hanging wall from an arbitrary vertical pin P. These bed lengths were used to define the dip of the fault in the footwall below the Weber Formation where there are no data.

In our solution the basement surface is folded in a south-facing kink band (fig. 18A) prior to the initiation of Willow Creek anticline. This kink band is encountered as the south dip found at the bottom of wells 8 and 9 of figure 17. This folding is probably caused by slip on a deeper fault, such as the basement fault that forms the Rangely anticline to the south. The timing of this folding is unknown and would have only a minor effect on the kinematics and shape of the main structure; it could have occurred before (as we assume), during, or after the Willow Creek anticline.

Our basic model begins as a triple junction that forms a drape anticline with $\theta = 41°$, $\phi = 19°$, $\epsilon = 101°$, and $\beta = 57°$ (fig. 18A, B). A fault-bend anticline (axial surface $\boldsymbol{b}$) forms over the site of the original triple junction in the basement. The basement for this and other fault bends is assumed to obey the constant-thickness fault-bend folding theory of Suppe (1983). The folding of the hanging-wall fault is handled with the theory of folding of preexisting faults of Suppe (1986). The anticlinal axial surface $\boldsymbol{aa'}$ of figure 18A is offset in figure 18B by interference with the developing steep limb; bedding-plane shear balance is maintained by transferring slip along bedding planes in the steep limb, such as the segment of $\boldsymbol{aa'}$ that parallels bedding (slip occurs instantaneously at the base of the Weber Formation in this stage of the model). The length of the basement surface has decreased by

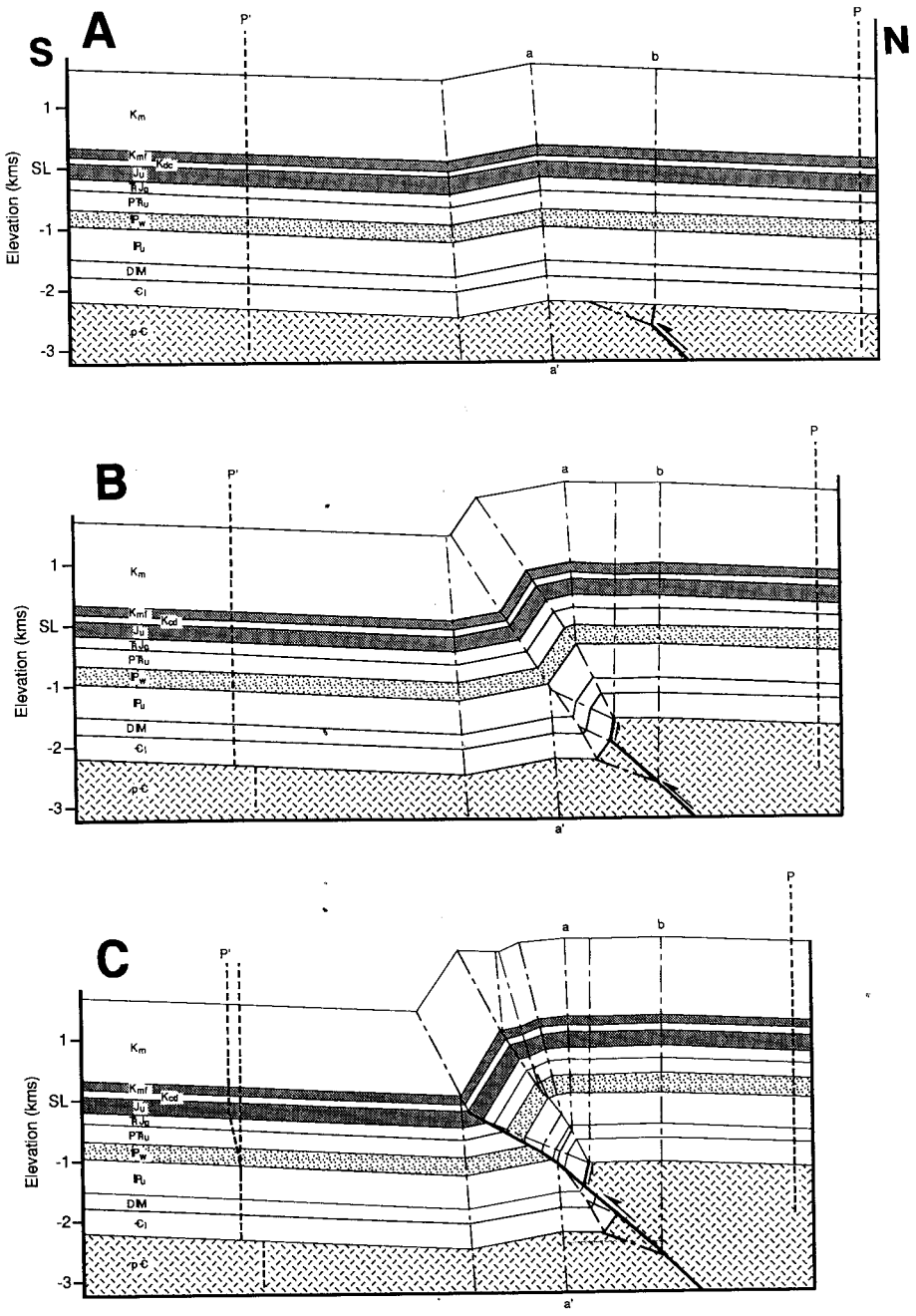

Fig. 18. Cross sections showing the kinematic sequence of development of the Willow Creek anticline, in same cross-sectional view as figure 17.

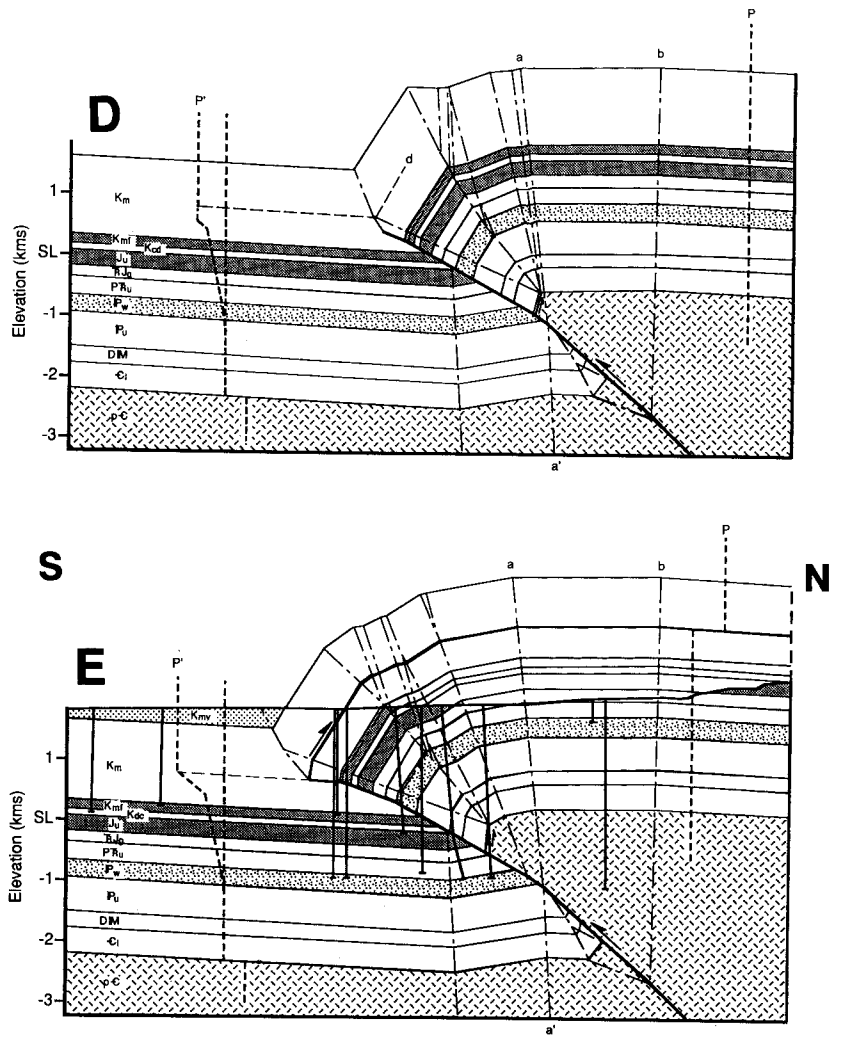

K_{mv} Mesaverde Group
K_m Mancos Formation
K_{mf} Mowry and Frontier Formation
J_u Jurassic Undivided (Carmel, Entrada, Stump, and Morrison Formations)
K_{cd} Cedar Mt. and Dakota Formations
TrJ_g Glen Canyon Formation
PTr_u Permian-Triassic Undivided (Chinle, Moenkopi, and Park City Formations)
P_w Weber Formation
P_u Pennsylvanian Undivided (Morgan Formation, Belden and Molas Shales)
DM Devonian-Mississippian Undivided (Chaffee and Madison Fms.)
C_l Lodore Formation
pC Basement (Uinta Mountain Gp. and Crystalline Rocks)

Fig. 18 (continued)

350 m as the original triple junction swept through the basement triangle, as illustrated in figure 18B by the offset of pin P' at the basement-cover contact. This slip could be consumed in several ways: 1.8 percent distributed shortening between Willow Creek anticline and Rangely anticline 19 km to the south, out of plane displacement along the oblique strike-slip fault in figure 16, or complex wedging to form kink band a'.

In figure 18C the main fault has propagated to the top of the Jurassic formations. Two anticlinal bends occur in the main fault, one of 5° at the top of axial surface a' and one of 7° at the center of the Weber Formation; these bends spawn additional axial surfaces that transmit shear to the top of the steep limb along bedding planes. As the main fault propagates up at gentler dip, simple shear parallel to bedding increases, as shown by the deformed pin line P'. The shear may exit the section up toward the anticlinal crest, opposite the direction of fold vergence, into the now-eroded upper strata of the anticline. Alternatively, it may exit toward the south, as suggested by the bending of pin line P', and be consumed in tectonic compaction or out-of-plane strain.

The fault propagates to the lower Mancos Formation in figure 18D. The fault dip decreases just above top of the Frontier Formation with an associated increased layer-parallel shear as shown by increased shear of pin P'; once again, this shear may exit at the eroded surface of the anticline. The deformation caused by this fault bend produces a transfer of shear parallel to bedding to form a degenerate kink band parallel to bedding within the Frontier-Mowry layer in the steeply dipping limb. At a shallower level, where this bedding-parallel axial surface intersects with an anticlinal axial surface (and flatter-dipping beds) a constant-thickness angular fold develops. Notice that as axial surfaces pass over upward-flattening fault bends there is an overall tendency for the structure to acquire a rounded shape.

The Willow Creek fault must flatten to a decollement (fig. 18E). There is significant fault displacement as high as the lower Mancos Formation, with Triassic strata juxtaposed against Mancos in well 6, yet there is no surface expression of a fault. The Mesaverde Formation is clearly unfaulted, and the Mancos Formation has the same stratigraphic thickness at the surface that it does in wells 1 and 2. Furthermore the surface syncline, also constrained by wells 3, 4, and 5, terminates at the Willow Creek thrust. We interpret this termination to be a wedge point as shown by the displacement of pin P. The wedge solution of figures 17 and 18 is not a geometric requirement for a kinematically-viable model. The same structural geometry can be obtained if the decollement were to transfer slip south along the near-horizontal Mancos decollement. If slip were translated to the south along this decollement, there should be evidence in the form of structures rooted at this level. However, surface geology (Cullins, 1969) and seismic data (Powers, 1986) show no structures at this level between Willow Creek anticline and Rangely anticline, 19 km to the south. If slip cannot go to the south, it must wedge back to exit at the erosion surface.

Structural wedges such as this are known in the frontal zone of the Rocky Mountains in Alberta (Price, 1981) and Wheeler Ridge anticline in southern California (Medwedeff, ms). Perry and others (1988) describe a similar wedge structure involving a Mancos decollement at the Grand Hogback monocline, near Glenwood Springs, Colorado, based on seismic and surface geologic data.

Stone (1986), in a regional study of the Uinta Mountain Group, shows greater than 2286 m of strata of the Uinta Mountain Group in the hanging wall of the Willow Creek structure. More recently he has come to believe, based upon additional well and seismic data, that rocks of the Uinta Mountain Group are about 1000 m thick in the hanging wall and thin or non-existent in the footwall (Stone, personal communications, 1988, 1992). Based on this extreme difference in thickness between the hanging wall and footwall, the Willow Creek thrust is probably a Precambrian, syndepositional normal fault against which strata of the Uinta Mountain Group accumulated. This fault was then reactivated as a thrust fault to form the Willow Creek anticline.

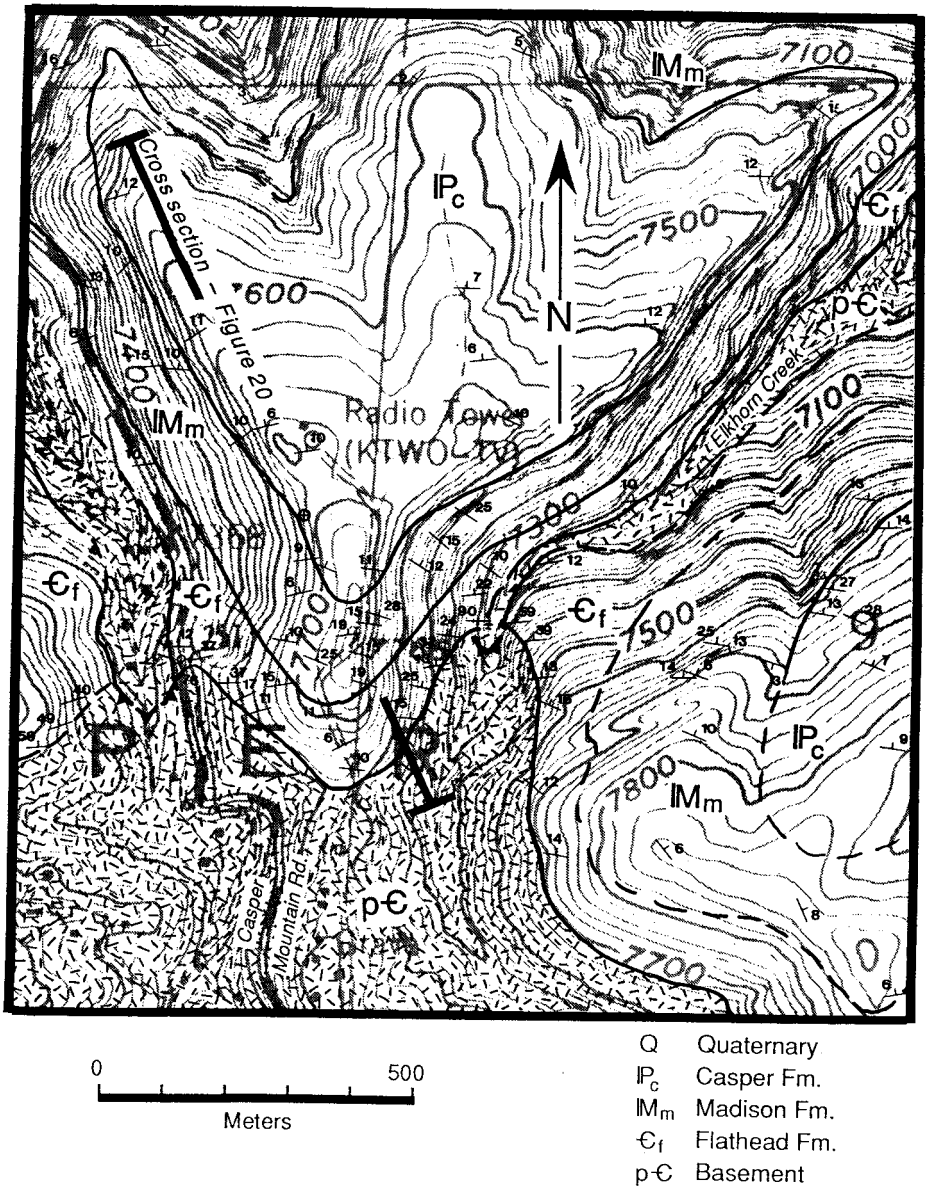

Fig. 19. Geologic map of a portion of Casper Mountain. Topographic base map is the Casper 1:24,000 USGS topographic quadrangle map.

Small Monocline on Casper Mountain

Summary.—A small basement-involved monocline of about 50 m relief is exposed in outcrop on the hanging wall of the main Casper Mountain structure south of Casper, Wyoming (fig. 19). This structural relief at the level of the basement-cover contact is accommodated by a narrow tight flexure with vertical beds in the Cambrian cover (figs. 20 and 21), similar to the prototypical model (fig. 1), whereas at the Madison level, 100 m higher, the relief is spread out over a broad flexure. This structure is modelled at the level of the basement-cover contact as a basement triple-junction with a drape anticline. The widening of the structure at higher levels is modelled as a wedge structure within the thickened syncline of the Flathead Formation (fig. 21).

Structural geometry.—A small, east-west trending monocline is exposed in the hanging wall of the main Casper Mountain structure south of Casper, Wyoming. Archean granite-gneiss is displaced along a thrust fault that is exposed in a road cut on the east side of Casper Mountain road and in outcrop along Elkhorn Creek (fig. 19). The fault dips south 33° at both outcrops (41° relative to regional dip). The cross section of figure 20 is a down-plunge profile projection of structural and stratigraphic data. The section shows that strata near the basement-cover contact dip more steeply than do strata at higher levels. Although the synclinal region of the Flathead Formation is not well exposed, the profile geometry shows that thickening must occur there. The fault in the basement disappears into this region of the cover. The broad, minor anticlinal bend about 100 m north of the fault in figure 20 is apparently unrelated to the structure under study.

The basement-cover contact is not exposed in the hanging wall, but its location is well constrained by soil mapping. The dip data in the cover shown in the enlarged area in figure 20 are from a resistant quartz-arenite marker bed that lies 10 m above the basement-cover contact; the shape of this marker bed and the basement-cover contact were surveyed with tape and altimeter. We interpret the unexposed steep basement-cover contact to be a fault, by analogy with the prototypical model (fig. 1) and the Big Thompson and Willow Creek anticlines.

The basement-cover contact in the footwall is exposed in a road cut on the Casper Mountain Road dipping 45° to 60° northwest. Here quartz-pebble conglomerate with clasts up to 3 cm diameter depositionally overlies weathered granite gneiss. In contrast the granite in the hanging wall, only a few centimeters away, is fresh and relatively unweathered. The pebbles in the Flathead Formation are cracked but show no evidence of faulting.

Direct evidence of how the basement deformed is incomplete due to limited exposure, and because the granite is not foliated in this area so rotation cannot be tested. The basement is well exposed south of the fault on Casper Mountain Road where it is fractured (see Narr, 1993) but not severely enough to suggest that the basement has been rotated to this vertical orientation, or that the cumulative offset on individual faults would produce this steep north end to the basement in the hanging wall (the mechanism suggested by Spang, Evans, and Berg, 1985). Furthermore the overall geometry is that predicted by the drape anticline triple-junction model.

Minor faults associated with the structure give an indication of the kinematics of its development; they are discussed in greater detail by Narr (1993). In the hanging wall at Casper Mountain Road the basement contains minor faults oriented approximately parallel to the main fault and show reverse slip. At the Elkhorn Creek site, where the footwall is exposed extensively in the creek bed, minor reverse faults also predominate, but they are oriented antithetic to the main fault. Strata of the Flathead Formation exposed in the

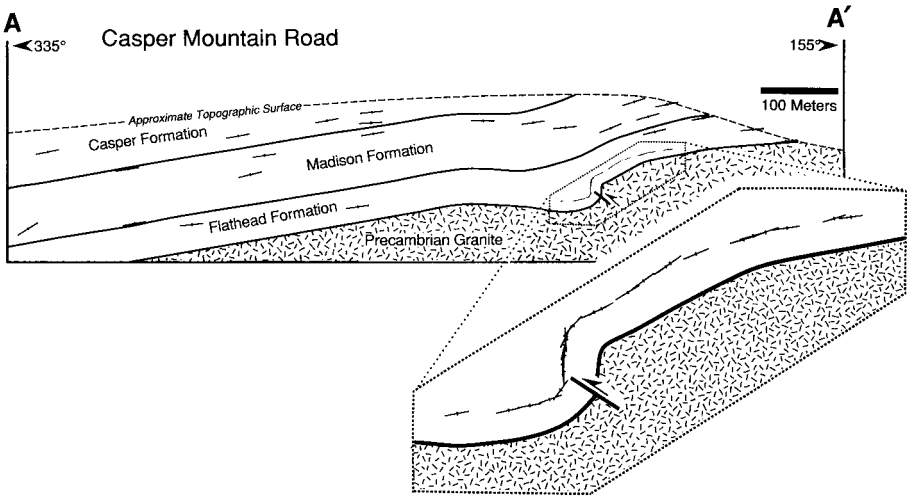

Fig. 20. Down-plunge projection of small monocline on Casper Mountain. The approximate surface trace is shown in figure 19; profile plane is oriented 155°/83°W. The enlarged insert shows attitudes measured along a single marker bed. Structural and stratigraphic data are projected less than 400 m from either side of the profile planes. Barbed bars show dip of bedding.

syncline at Casper Mountain Road show layer-parallel shortening and crowding in the syncline, with faults dipping mainly antithetic to the main fault.

Retrodeformable structural interpretation.—Figure 21 is a retrodeformable cross section in the profile plane of *AA′* (fig. 20). The relatively gentle folds in basement of the hanging wall are computed as constant-thickness fault-bend folds (Suppe, 1983). The main fault and the steep basement-cover contact in the hanging wall are interpreted as the two fault branches of a drape anticline triple junction. The dipping basement-cover contact exposed on the Casper Mountain Road is interpreted as the top of the prism of deformed basement in the footwall. This structure is at a stage of development equivalent to figure 1C. The model parameters of this triple junction are: $\theta = 41°$, $\phi = 20°$, $\beta = 45°$, and $\epsilon = 92°$.

The main anticline of the structure, which formed above the steep fault branch, is a drape fold (fig. 21). A structural wedge in the Flathead Formation acts to thicken the syncline, to reduce the dip of the overlying strata, and to transfer slip upsection to a decollement at the base of the Madison Formation. The offset vertical line at the left side of the section is an offset pin line.

Due to little outcrop there is no direct field observation of the single fault used to model the thickened Flathead syncline. Numerous minor antithetic faults are exposed in outcrops within the syncline and probably represent the actual mechanism by which synclinal thickening occurs. It is probable that synclinal thickening occurs on a number of faults, each slipping proportionately less that the single fault of this model. A single fault was used in the model for kinematic simplicity.

In the following three case studies we qualitatively compare their geometry with the predictions of the triple junction model of basement-involved structures. Their qualitative similarities to the predictions of the

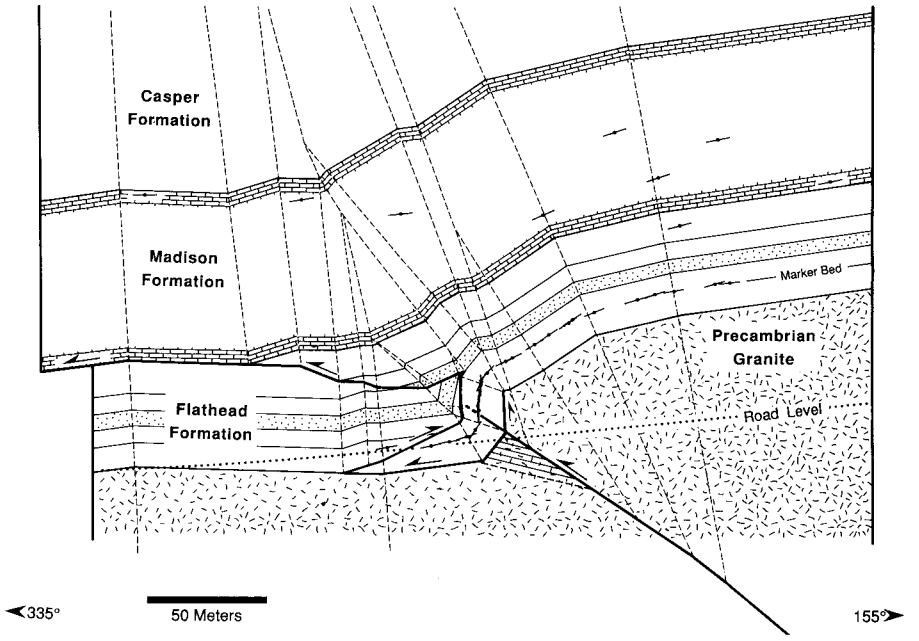

Fig. 21. Retrodeformable cross section of small monocline on Casper Mountain, in same profile plane as figure 20.

model support the general triple-junction theory. In particular Rattlesnake Mountain and Banner Mountain anticlines provide fairly direct outcrop observation of the near vertical drape-induced detachments between basement and cover, which are a key property of the drape anticline triple-junction model. Five Springs anticline displays strong disharmonic folding between basement and cover which is analogous to the drape-induced detachment and kink-band interference of our prototypical model (fig. 1).

Rattlesnake Mountain Anticline

Summary.—Exposures of the Rattlesnake Mountain anticline along the canyon of the Shoshone River, Wyoming (fig. 22) give a direct view of the steep fault between unfolded basement and folded cover that is central to the drape anticline triple-junction model (fig. 1). This exposed fault has additionally broken through the cover along two branches, probably associated with late-stage stretching of the steep limb (compare fig. 1D). In spite of these complexities, a drape detachment fault appears to be a key aspect of the Rattlesnake Mountain anticline.

Surface structural geometry.—Many geologists consider Rattlesnake Mountain anticline, west of Cody, Wyoming, as the type example of a basement-involved structure (see Stone,

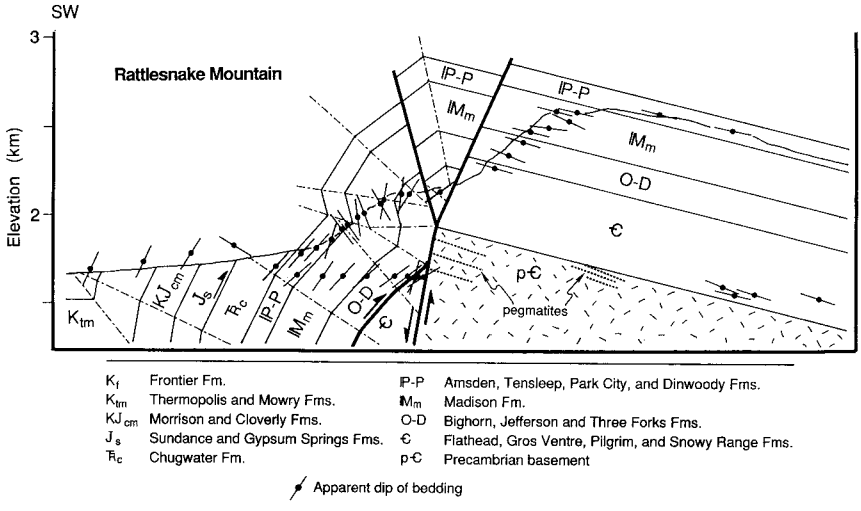

Fig. 22. Cross section of near-surface structure of Rattlesnake Mountain anticline, based on traverses near Shoshone Canyon, Wyoming. An early contractional fault along the base of O-D is utilized in part by a later, drape-induced detachment fault that has broken through the cover strata. The basement is not folded.

1984). Near the Shoshone River Canyon, Paleozoic cover can be seen draping over the uplifted edge of granitic basement to form this anticline (Pierce, 1966; Pierce and Nelson, 1968).

Stearns (ms) argues that the basement at Rattlesnake Mountain anticline acted as a rigid indenter and experienced no rotation in the anticline. He argues that, except for a narrow fault zone, basement shows minimal sign of brittle internal deformation and was undeformed during growth of the anticline. Narr (1993) verified Stearns' field evidence and agrees with this interpretation.

A set of parallel, gently dipping, Precambrian pegmatite dikes is present in the basement adjacent to steeply-dipping strata on the southwest side of the anticline, parallel to similar dikes beneath gently-dipping strata on its northeast limb (fig. 22). Likewise, northeast of the normal fault that emerges from the apex of the basement, strata are planar and show no sign of folding above the exposed basement (fig. 22).

Kinematic indicators in cover.—The basement-cover contact on the southwest side of the anticline is a steep, southwest-dipping, normal fault (fig. 22). Cambrian strata here have been thinned to about 20 percent of their normal thickness due to layer-parallel extension. At a road cut on Route 14–20 through the steep limb of the structure, minor faults are present in the Cambrian Grove Creek Formation. An analysis of these faults, based upon the *P-T* right-dihedra method of Angelier and Mechler (1977), indicates that the principal shortening direction plunges approx 30° northeast, nearly normal to bedding, and principal extension is parallel to bedding (Narr, ms).

These results are in general agreement with the shortening and extension directions found in strata at this structural position, relatively low in the cover sequence in the steep limb, at Casper Mountain. These results contrast with the interpretation of minor faults in the steep limb of the structure at Five Springs, discussed below, where layer-parallel shortening is indicated.

Toward the southeast end of Rattlesnake Mountain anticline, on Cedar Mountain, where the structure begins to plunge steeply to the southeast, strata in the steep limb have been tectonically thickened due to thrust repetition rising from a decollement near the base of the Ordovician, and a rabbit-ear fold is developed at the top of the steep limb. It is likely that this same steep-limb shortening has occurred along other parts of Rattlesnake Mountain where exposures are less complete. Evidence is seen in figure 22: if the structure is restored such that the upper surface of the Cambrian is continuous, Ordovician and younger strata would exhibit excess bed length. This suggests that a decollement may be present between the Cambrian and Ordovician that transported the younger strata up the steep limb prior to the extensional offset of the Cambrian. This evidence of layer-parallel shortening higher in the cover sequence is seen likewise at Five Springs and supports the assertion made in the discussion of Five Springs, below, that stretching is more common at lower levels in the cover, whereas thickening is more common at higher levels (compare higher levels of fig. 1).

Some overturning is seen in figure 22, but at sites northwest of the Shoshone River Canyon exposure, nearly the entire steep limb is overturned. Such strong overturning raises the possibility that the main fault underlying the hanging wall dips moderately to the northeast (compare lower levels of fig. 1D).

Discussion.—The seeming contradictory structural features at Rattlesnake Mountain—extension at the anticlinal crest and at low stratigraphic levels in the steep limb, a near-vertical fault along Shoshone Canyon, and layer-parallel shortening and overturning in the steep limb—are consistent with predictions of the drape anticline triple junction model. The steep fault shown in most cross sections of Rattlesnake Mountain along Shoshone Canyon (Stone, 1984) is interpreted as the upper branch of a basement triple junction.

Banner Mountain Anticline

Summary.—Exposures of Banner Mountain anticline on the canyon walls of Lower Deer Creek, Wyoming (figs. 23 and 24), are consistent with a drape-induced detachment, although the steeply dipping basement-cover fault contact is not exposed. The cover in the steep limb has undergone dip-parallel extension and thinning. The basement did not rotate during formation of the anticline, although a Precambrian fold is present that may have localized the basement triple-junction. The main, Deer Creek thrust dips gently to moderately toward the south-southeast. The near-surface geometry of Banner Mountain monocline is consistent with a drape anticline that has broken through the cover, similar to the model of figure 1D. A sub-thrust basement cored anticline is also present.

Surface structural geometry.—Banner Mountain anticline is an east-northeast trending monocline at the northern margin of the Laramie Range in Wyoming (figs. 11 and 23). This structure is in the hanging wall of the Deer Creek thrust, which transports basement and cover strata northward over the Powder River basin (fig. 24). In contrast with other structures we have presented, the Deer Creek thrust displays substantial structural relief in the footwall as indicated by basinward dips for over a kilometer south of the fault trace and an estimated 2+ km depth to basement in a well 4 km to the north (figs. 23 and 24). Little is known of this footwall structure, which makes structural modelling speculative; however the details of the hanging wall exposed on the mountainside of Lower Deer Creek Canyon are enlightening, because the basement edge is exposed (fig. 24).

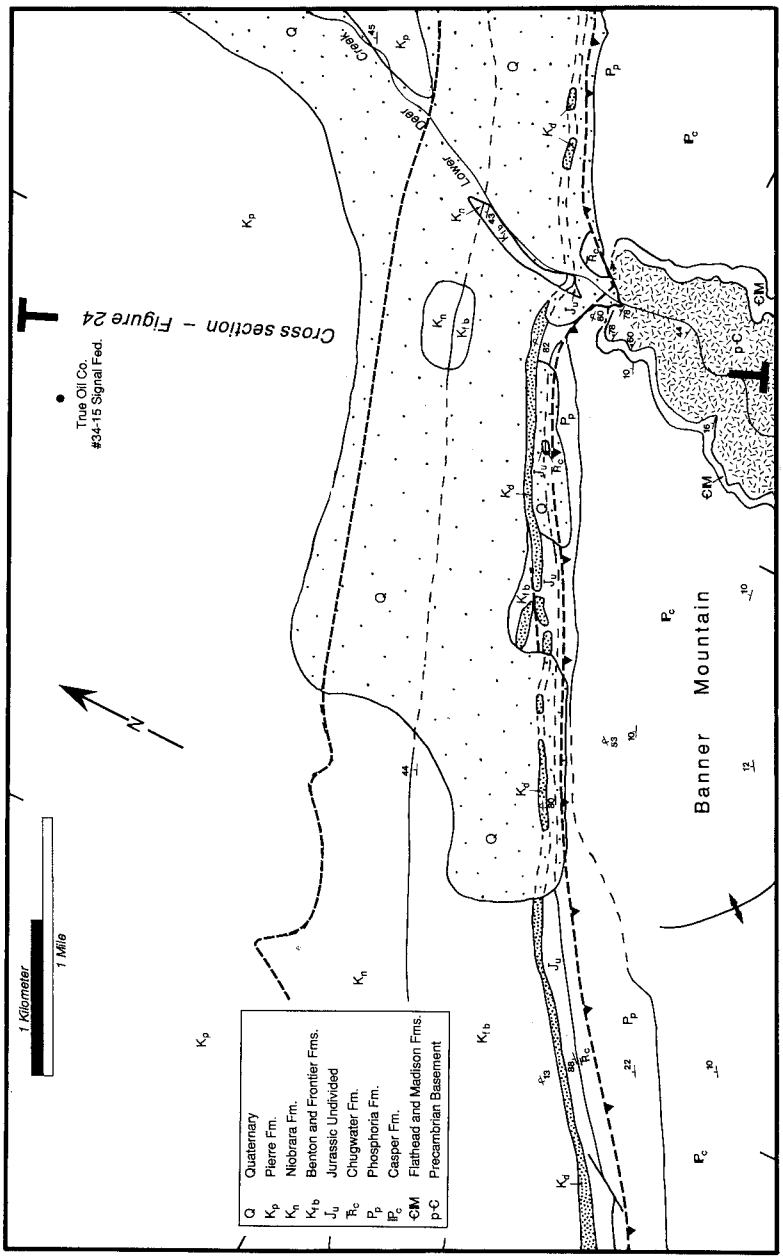

Fig. 23. Geologic map of Banner Mountain area, after Berryman (1942), Sears (1949), and Narr (1990).

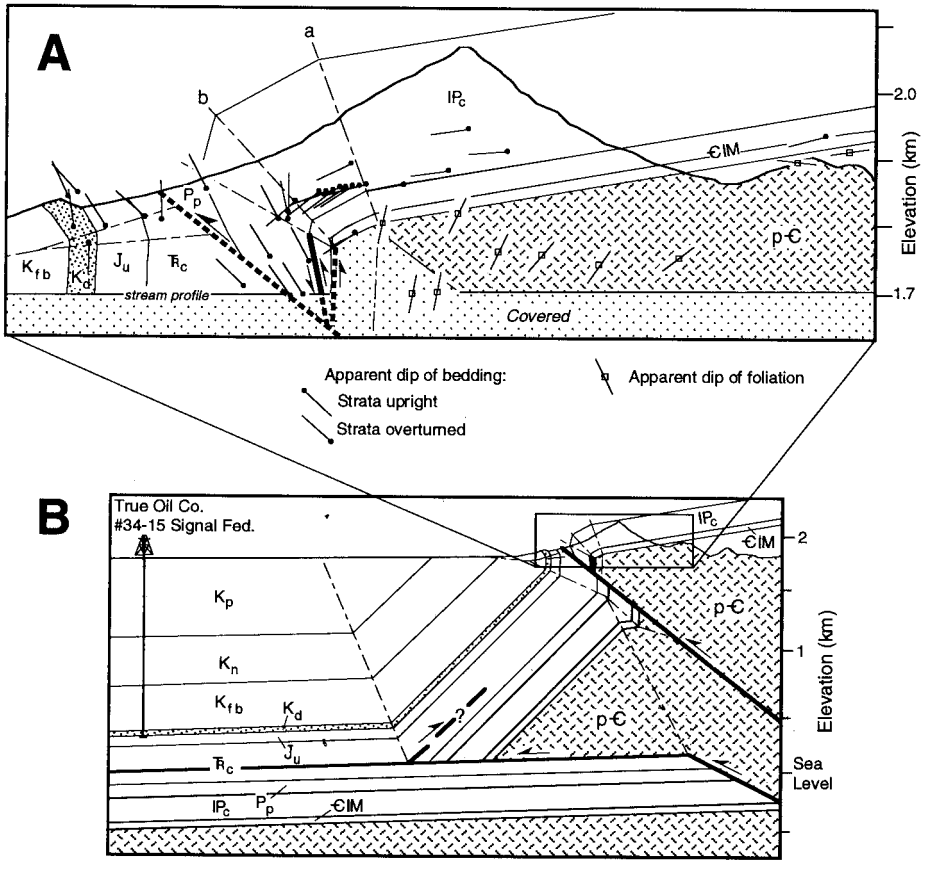

Fig. 24. Cross section of near-surface structure of Banner Mountain monocline. See figure 23 for location and for explanation of formation symbolism.

The basement in Lower Deer Creek Canyon is weakly- to moderately-foliated granite and granitic gneiss which shows a folding of this foliation (fig. 24). This folding is Precambrian in age because the angle between the foliation and the unconformity varies systematically from south to north where the unconformity has a constant 10° north dip (south of axial surface *a*, fig. 24). In contrast, where the strata above the unconformity are rotated by 26° across axial surface *a* the foliation in the basement exhibits little change in dip. Therefore the folding of the basement between axial surfaces *a* and *b* is interpreted to be produced by shear parallel to the foliation.

The basement-cover contact at the north end of the basement (north of axial-surface *b*) is a near-vertical fault that is nearly parallel to foliation in the basement. The Flathead Formation is absent in the steep limb of the monocline, and the Madison Formation has been tectonically thinned from axial surface *b* to the base of its exposure in the steep limb. Minor faults in the Madison Formation of the steep limb indicate extension parallel to the dip of bedding. Thus we see that the steep fault between basement and cover that was

proposed for previous structures is clearly exposed on the walls of Lower Deer Creek Canyon, as well as at Shoshone Canyon (fig. 22). For this reason we interpret the Banner Mountain structure also to be formed as a drape anticline triple junction.

Dip of the Deer Creek thrust.—The fault surface of the Deer Creek thrust is not exposed in outcrop; however, the map pattern of Berryman (ms) and Sears (ms) suggest a moderate ($\approx 30°$) dip. Based on Narr's (ms) mapping the fault dips south-southeast about 38° in the profile plane of figure 24. The thrust nature of this margin of the Laramie Range is also confirmed by several wells located 14 km east which penetrate basement in the hanging wall and cross a fault into Cretaceous strata in the footwall (Curry and Curry, 1972).

A gravity survey was done by Narr (ms) to constrain dip of the Deer Creek thrust. The gravity data are not very sensitive to fault dip, but they rule out large amounts of low density Mesozoic strata in the footwall of the Deer Creek thrust. Likewise, the gravity data may be used to constrain the fault dip to less than 45°. The model of figure 24B shows a deep basement-involved structure in the footwall of the Deer Creek thrust. This interpretation is based on both gravity and local geology. A possibly similar structure was drilled 11 km east of Lower Deer Creek Canyon in the Texaco-Government/Rocky Mountain Exploration #1 well (T32N R76W Sec 12) which was drilled 2.5 km south of the thrust front to a depth of 2791 m. The well penetrated only crystalline basement, which could result from a stacking of basement-involved structures similar to that shown in figure 24B.

Five Springs Anticline, Bighorn Mountains

Summary.—The Five Springs area of the western Bighorn Mountains in Wyoming (fig. 25) has a basement-cored anticline of similar magnitude and shape to the Willow Creek anticline but is exposed at the level of the basement-cover contact (compare figs. 17 and 26). Both structures have approx 2 km of structural relief and have an interlimb angle of about 90° at the Cambrian level. However, at higher stratigraphic levels the steep limb at Five Springs becomes strongly overturned with dips reaching as low as 35°. This detached folding of the cover is interpreted to be a result of interbed shear of the sort deduced to exit the erosion surface in the analysis of Willow Creek anticline (figs. 17 and 18). The bedding-parallel faults that transmit this shear have a spacing of about 40 m in the massive Paleozoic carbonates. The dip of the near-surface segment of the main Five Springs thrust is approx 20°, based on gravity modelling and overturned bedding dips of 10° to 30° near the mapped fault trace. Outcrop study of preexisting structures in the basement shows rotation of 40° to 50° (fig. 26), but no evidence exists for folding of the basement unconformity to the 80° overturned dip of the Cambrian cover (Wise, 1964; Hoppin, 1970; Narr, 1993). Therefore a steep drape-induced detachment between basement and cover is consistent with the data, and the drape anticline triple-junction model seems viable.

Surface structural geometry.—The Five Springs monocline lies along the west side of Bighorn Mountains in Wyoming (fig. 11) and has an approximately horizontal fold axis trending northwest (fig. 27). Figure 26 is a cross section that summarizes most observations that constrain the near-surface structure. Toward the interior of the range to the northeast, bedding dips 4° southwest. Granitic basement is exposed in the anticlinal hinge, across which bedding in the basal Cambrian becomes steep to overturned. Higher stratigraphic levels are strongly overturned with dips reaching as low as 35°, but this overturning appears to be detached judging by excellent mountainside exposures which show an angular

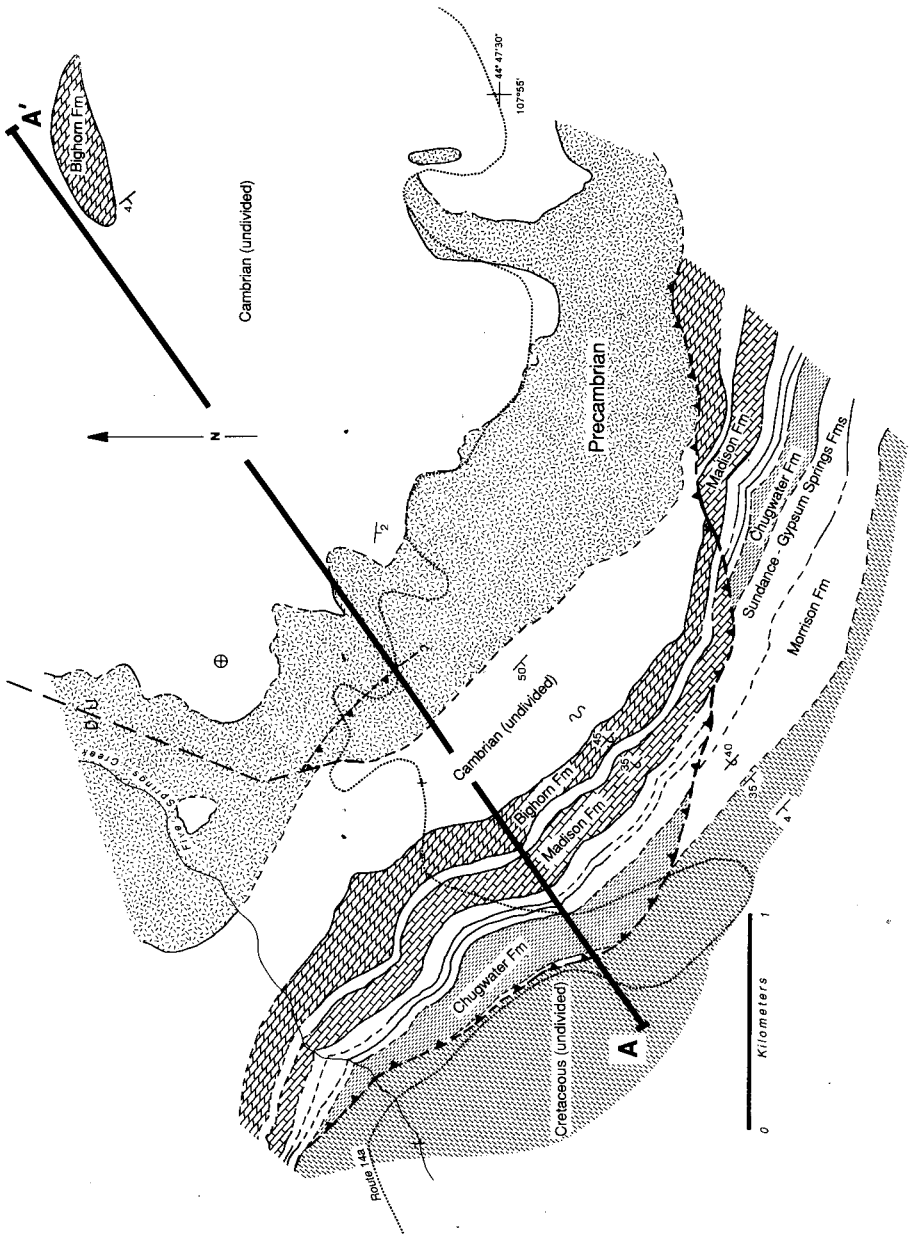

Fig. 25. Geologic map of the Five Springs area, from Hoppin (1970) and Narr (1990).

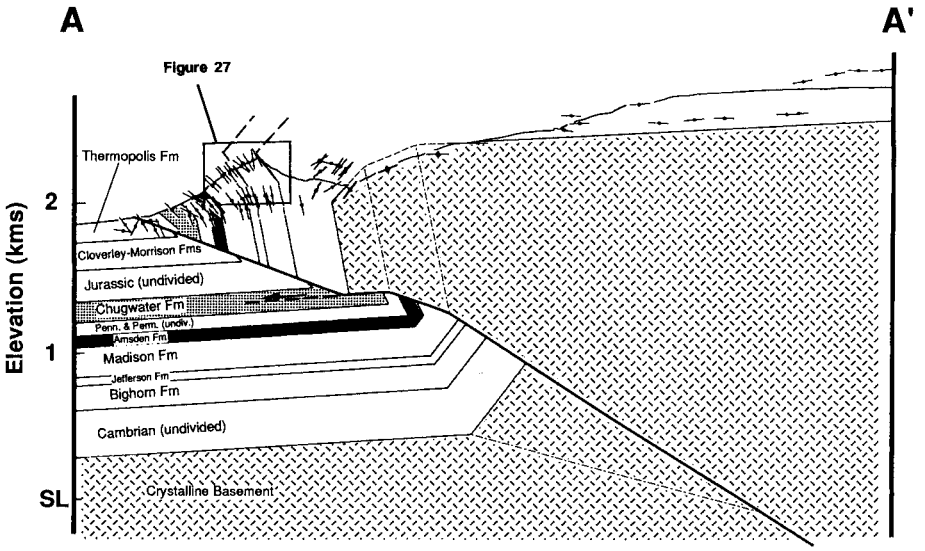

Fig. 26. Cross section of Five Springs monocline (loc. on fig. 25). Structural attitudes indicated are apparent dips in plane of cross section. Dips indicated for basement show relative rotation from horizontal, interpreted from rotation of pegmatite dikes (Narr, 1993).

anticline in the Bighorn Formation that is detached from steeply-dipping older strata (fig. 27). This detached folding requires shear of the steep limb out of the syncline similar to that deduced from deformed pin lines at Willow Creek anticline (fig. 18) or to that resulting from kink-band interference in stage *c*, our prototypical model (fig. 1C.1). This would be a "rabbit-ear" fold in the terminology of Brown (1984). The bedding faults required for this shear were studied by Narr (ms) who found that their spacing in the Bighorn and Madison Formations average about 40 m.

The steep basement-cover contact on the west side of the fold hinge is not exposed, so it is not known whether the basement has experienced the same 90° of rotation as the strata. The steep basement-cover contact is likely a fault similar to Big Thompson and Willow Creek anticlines, Casper Mountain, Rattlesnake Mountain, and Banner Mountain (figs. 13, 17, 18, 21, 22, and 23) and similar to our prototypical model (fig. 1). Or the unconformity could be fully folded. By measuring sub-parallel, Precambrian pegmatite dikes in a series of traverses across the basement exposed in the fold hinge, Narr (1993) demonstrates that basement has been rotated 40° to 50° about the Laramide fold axis (shown as the dip symbols in the basement in fig. 26). This magnitude of folding of the basement is similar to Willow Creek anticline (fig. 17). Our structural solution assumes the steep contact is a fault as predicted by the drape anticline triple-junction model.

Dip of the Five-Springs thrust.—The Five Springs thrust fault is located at the base of the steep limb, with gently southwest-dipping Cretaceous strata below the thrust. We were unable to make direct observation of the fault dip in this area. However, beds adjacent to the thrust are strongly overturned, dipping 10° to 30° northeast, and may record the approximate fault dip. At a site 550 m south of Five Springs Creek the strata of the Chugwater Formation are overturned and dip 16° northeast. Just southwest of here the

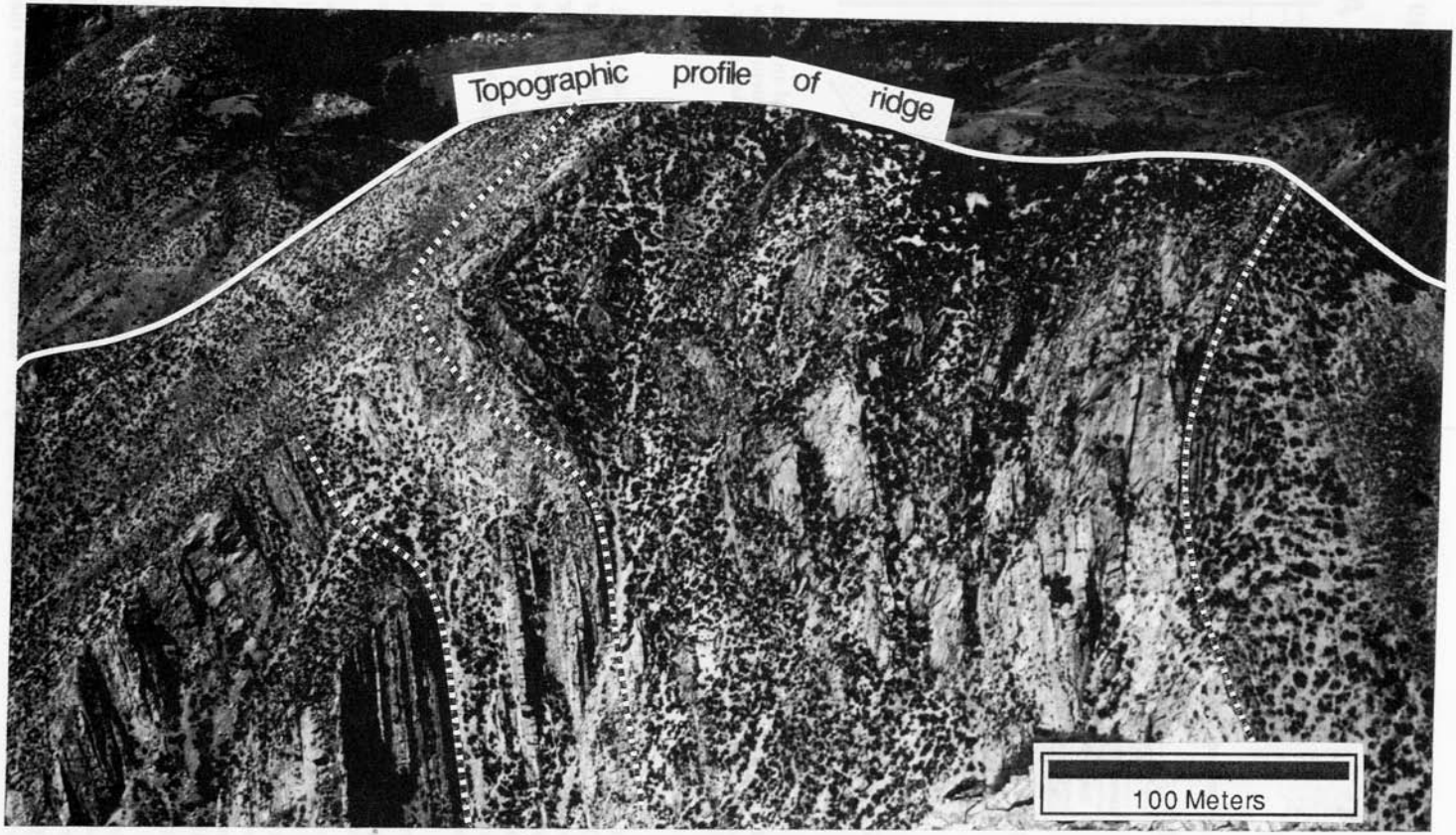

Fig. 27. Photograph of angular detached fold in Bighorn Formation in steep limb of Five Springs monocline. Location of photograph is shown in figure 26.

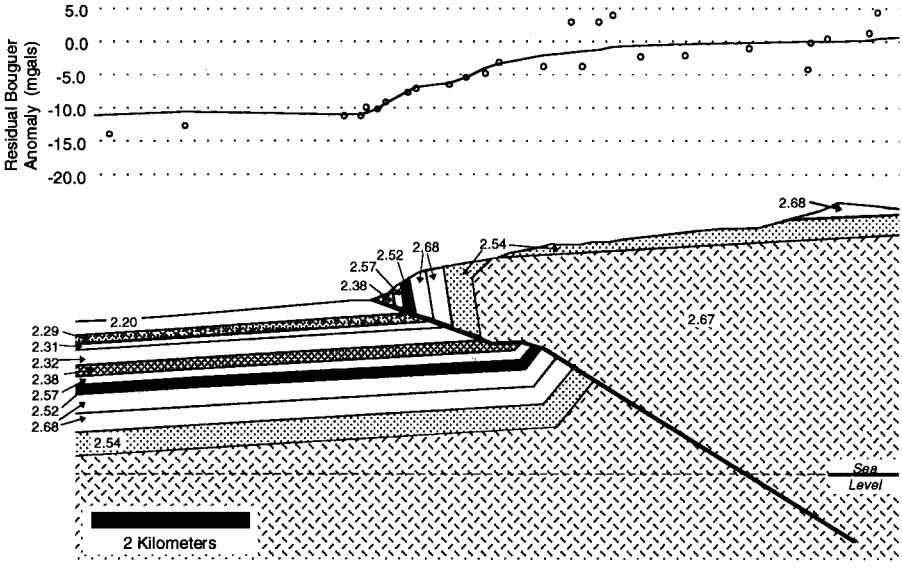

Fig. 28. Residual Bouguer anomaly of Five Springs area along same profile plane as figure 26. Open circles are based on measured data; solid curve is computed based on the model beneath the graph. Densities are in g/cm^3. A linear regional gradient was removed by inspection. Survey details and principal data are given in Narr (ms).

Sundance Formation shows a number of slickensided surfaces with average dip 25° northeast. The slip vectors are in the dip direction, and although the sense of slip is indeterminate it is presumably southwest-directed thrusting.

The only direct exposure of the fault is southeast of the line of cross section where the strike of the fault swings around to become east-northeast, nearly parallel to the line of cross section, where Hoppin (1970) shows the fault as a left-lateral tear. The exposed fault plane dips 42° toward north-northwest with striae parallel to the dip direction. This slip direction indicates movement of the hanging wall oblique to the presumed transport plane (normal to the fold axis) and to the slickensides at the base of the steep limb. This slip direction also disagrees with the direction of shortening interpreted from minor faults in basement, which indicate that shortening is horizontal and perpendicular to the fold axis (Narr, 1993). Furthermore, minor faults within the steep limb indicate shortening in the dip direction (Narr, ms). We conclude that the striae on the exposed fault surface result from non-coeval or non-plane strain at this site.

A gravity survey by Narr (ms) also constrains the dip of the thrust fault to 20° (±5°) at shallow depths. Figure 28 gives a gravity model (solid curve) of the Five Springs range front with the observed gravity as open circles. The scatter of data in the hanging wall reflects variability of the gravity field that does not trend parallel to the fold axis. In modelling we optimized the fit to the structure where the fault is nearest to the surface, both because this is where the gravity response is most sensitive to fault dip because high-density Paleozoic and basement rock overlies lower-density Cretaceous strata, and because the data are projected the shortest distance to the trace of the cross section.

Structural interpretation.—Summarizing the key structural constraints of the central part of the Five Springs monocline: (1) Near-vertical, planar beds in the steep limb suggest a

near-vertical southwest basement-cover contact in the hanging wall. This steep contact may be a fault by analogy with Big Thompson and Willow Creek anticlines, as well as our interpretation of Casper Mountain anticline. (2) The basement in the hanging wall has rotated along with the cover by 40° to 50°, somewhat higher magnitude than Willow Creek and Casper Mountain anticlines. (3) The Five Springs thrust dips about 20° toward northeast, based on strongly overturned dips adjacent to the fault and interpretation of gravity data. This is 24° relative to the regional southwest dip. (4) The overturned detached structure in the hanging wall requires out of the syncline shear.

These geometric constraints were used to model the kinematic behavior of basement during the development of the Five Springs monocline (fig. 29). In its initial phase (fig. 29A) a drape anticline develops at triple junction *TJ1*. The hanging wall slips forward along the fault, deforming a triangle of basement in the footwall ($\theta = 36°$, $\epsilon = 82°$, $\phi = 18.5°$, and $\beta = 50°$). The main fault dips more gently above triple junction *TJ2* (fig. 29C). As the basement reaches about the level of the Chugwater Formation *TJ3* forms, and the basement begins to slip along a bedding plane decollement (fig. 29D). The active axial surfaces located at *TJ2* and *TJ3* produce the observed 40° to 50° folding of the basement-cover unconformity.

DISCUSSION

Basement-involved structures show diverse geometry and seemingly contradictory evidence of their deformational history, which has been a major obstacle to the development of a useful, quantitative understanding. This diversity has led seasoned investigators to comment: "There is no one single structural style in the Wyoming foreland." (Brown, 1988, p. 22), and "No one model will fit all cases, as I'm sure you will agree." (Hansen, 1984, p. 73). Nevertheless the main obstacle to understanding has been the combination of structural diversity with large size and consequently limited exposure of any single structure. We have attempted to overcome this problem through six relatively well constrained case studies.

The small monocline on Casper Mountain (figs. 19–21) presents a nearly complete view of a basement-involved structure. At Willow Creek anticline the combination of well data and surface geology places tight constraints on the geometry of the structure (figs. 16-18). The plunging nature of Big Thompson anticline provides an oblique cross section that extends from the basement to the upper levels of the cover, and the addition of gravity data further constrains the geometry (figs. 12-15). More limited views are presented of the three other structures. Rattlesnake Mountain (fig. 22) and Banner Mountain anticlines (figs. 23-24) provide mountain-side observation of drape-induced detachments, which are a key element of all our case studies. Five Springs anticline provides key mountainside evidence for disharmonic folding between basement and cover (figs. 25-29). The key features of these structures are summarized in table 2.

A variety of triple junction structures are kinematically viable and seem capable of explaining much of the observed diversity of basement-involved structures, particularly when combined with a detachment between basement and cover. This conceptual model was tested successfully by retrodeformable modelling of three structures (figs. 13, 15, 17, 18, 20, and 21).

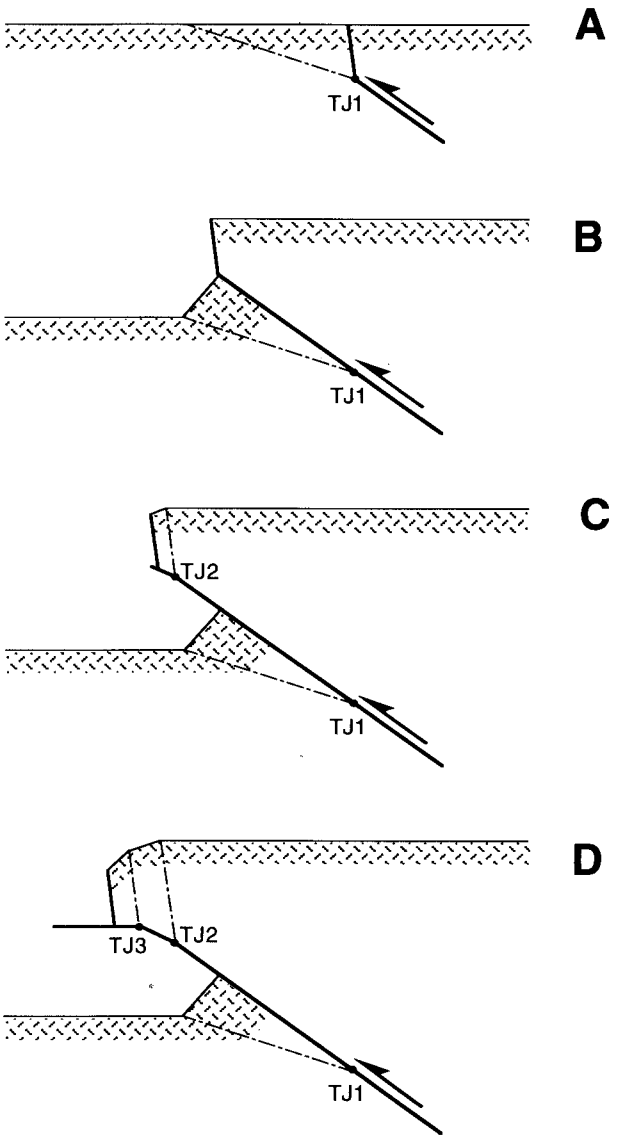

Fig. 29. Triple-junction model of basement structure in the evolution of the Five Springs monocline.

Triple junctions may develop as an upward-propagating thrust fault encounters some preexisting weak surface such as a fault, deep joint, or lithological boundary that will almost certainly lie at an oblique angle to the deep fault. If slip initiates on this preexisting oblique feature, then the formation of a triple junction is a geometric necessity. Whether interac-

TABLE 2

Summary of principal geometric elements of the basement-involved structures studied

Structure	Shape	Maximum Rotation of Basement (evidence)		Fault Dip, Relative to Regional Dip (type)		Upper Termination of Main Fault	Deformation in Cover *("Dip" refers to bedding attitude)*
		Hanging Wall	Footwall	Main Fault	Shallow-Level Fault		
Casper Mountain	Monocline	25° (cover strata)	35°-50° (cover strata)	41° (thrust)	88° (normal)	Disappears in cover (decollement likely)	Dip-parallel shortening in syncline. Drag folds with same shear as shallow fault.
Big Thompson Anticline	Monocline	None (foliation)	?	35° (thrust)	70° (reverse)	Disappears in cover	Dip-parallel shortening (lift-off fold in anticline). Dip-parallel extension in steep limb.
Willow Creek Anticline	Monocline	35° (dipmeter, cover strata)	?	41° (thrust)	79° (normal)	Decollement (structural wedge?)	None ?
Five Springs	Monocline	45°–55° (pegmatite dikes)	?	24° (thrust)	82°? (reverse?)	Surface break	Dip-parallel shortening (lift-off fold in steep limb). Out-of-syncline bedding plane slip.
Banner Mountain	Monocline with 8° forward dip	26° (cover strata) 15°–20° (foliation)	?	40°–55° (thrust)	77° (normal)	Surface break	Dip-parallell extension in steep limb.
Rattlesnake Mountain	Monocline with 15° back dip	None (pegmatite dikes)	?	?	80° (normal)	Disappears in cover (minor surface break)	Dip-parallel extension near cover/basement contact and near anticline axial surface. Shortening in steep limb.

tion with any individual preexisting weak surface develops into an important triple junction is a function of the geometry of the junction and the relative strength of the preexisting surface. This paper takes an exclusively two-dimensional view of the triple junction model; in three dimensions, a triple junction forms a line or curve in space. In general the preexisting surface will not strike parallel to the deep fault, consequently the triple junction line will have a plunge, and the resulting structure will be non-cylindrical.

A triple junction will form in association with any non-planar fault. A non-planar fault may result whenever a fault propagates through a zone where the regional stress field is locally perturbed, as may occur near a material interface such as the basement-cover contact. Such a situation could, for example, develop a listric fault, which might then form a drape anticline as fault displacement increases.

Low-temperature, basement-involved, compressive structures that occur in many mountain belts can be modelled quantitatively in two dimensions by the kinematics of triple junctions. A moderately dipping deep fault bifurcates into two branches as it approaches, or reaches, the basement surface. In particular, the model of figure 1 represents perhaps the most common general solution for the steeply-dipping monoclinal portions of these structures. In this model a moderately-dipping fault bifurcates upward into a steeper fault and a more gently dipping axial surface. In general the kinematic sequence of the cover predicts an early phase of layer-parallel shortening, followed by a later phase of extension.

Fault-bend folds that conserve layer thickness (Suppe, 1983) are one special case of the allowable triple-junction geometry. The kinematics of triple junctions are not confined to application with basement-involved structures but can operate whenever a structural configuration involves interacting faults or faults that change attitude. Nor is the triple-junction model confined only to thrust and extensional regimes. Its geometry applies also to true three-dimensional deformation, such as areas experiencing a combination of strike-slip faulting and thrusting (for example, Abers and McCaffrey, 1988; Shaw, Bischke, and Suppe, 1994).

CONCLUSIONS

During compressive deformation in the brittle upper crust the interaction of non-planar fault segments generates fault-bend folds in adjacent basement rock. The kinematics of these volume-constant fault-fault-fold triple junctions can be used to model the formation of basement-involved compressive structures. Of the six possible fault-fault-fold relationships, four are likely to operate in the upper crustal brittle regime to produce drape anticlines, fault-bend anticlines, fault-bend synclines, and wedge structures.

Well-layered sedimentary rocks can have a complex kinematic history in response to the evolving basement structures that underlie them. The drape folds that are characteristically associated with basement-involved structures apparently form above triple junctions in the base-

ment. Their structural evolution can be complex. Layer-parallel shortening is common during the early stages of kinematic development of a basement-involved structure, whereas extension is more common during more advanced stages of their kinematic history.

It is the compounding of fault-fault-fold triple-junctions in the basement, which are controlled in part by pre-existing inhomogeneities, and their interaction with the stratified cover, that gives rise to the complex and diverse geometries characteristic of basement-involved structures.

ACKNOWLEDGMENTS

We wish to thank Laurel Pringle-Goodell and Helen Syms for helping with geological field work. We are grateful to the many people who shared ideas, read early drafts of the manuscript, and otherwise assisted us, including: Dick Bischke, Bill Bonini, Steve Hook, Lois Koehnken, Neil Lundberg, Don Medwedeff, Jason Morgan, Jon Mosar, Van Mount, Laurel Pringle-Goodell, Don Stone, and Hongbin Xiao, as well as many others. The paper benefitted from thoughful reviews by E. A. Erslev, R. H. Groshong, Jr., John Rodgers, and D. S. Stone.

Generous financial support for this research was provided by the following institutions: Texaco Exploration and Production Technology Division, Mobil Exploration and Production U.S. Inc., Sigma Xi (Grant-in Aid of Research), Chevron U.S.A., and Geological Society of America (Grant No. 3838-87). Fellowship support (for Narr) was provided by Amoco Foundation and Sun Oil Co. Page charges for this article were paid for by Chevron Overseas Petroleum Inc.

This study is part of Narr's Ph.D. thesis research, done at Princeton University.

REFERENCES

Abers, G., and McCaffrey, R., 1988, Active deformation in the New Guinea fold-and-thrust belt: Seismological evidence for strike-slip faulting and basement-involved thrusting: Journal of Geophysical Research v. 93, p. 13,332–13,354.

Allmendinger, R. W., Ramos, V. A., Jordan, T. E., Palma, M., Isacks, B. L., 1983, Paleogeography and Andean structural geometry, northwest Argentina: Tectonics, v. 2, p. 1–16.

Angelier, J., and Mechler, P., 1977, Sur une méthode graphique de recherche des contraintes principales également utilisable en tectonique et en séismologie: la méthode des diédres droits: Bulletin de Societie Geologique de France v. 19, p. 1309–1318.

Angelier, J., Colletta, B., and Anderson, R. E., 1985, Neogene paleostress changes in the Basin and Range: A case study at Hoover Dam, Nevada-Arizona: Geological Society of America Bulletin v. 96, p. 347–361.

Avouac, J. P., Beyer, B., and Tapponnier, 1992, On the growth of normal faults and the existence of flats and ramps along the El Asnam active fold and trust system: Tectonics, v. 11, p. 1–11.

Barazangi, M., and Isacks, B., 1979, Subduction of the Nazca plate beneath Peru: evidence from spatial distribution of earthquakes: Royal Astronomical Society Geophysical Journal, v. 57, 537–555.

Beckwith, R. H., 1941, Structure of the Elk Mountain district, Carbon County, Wyoming: Geological Society of America Bulletin, v. 52, p. 1445–1486.

Berg, R. R., 1962, Mountain flank thrusting in Rocky Mountain foreland, Wyoming and Colorado: American Association of Petroleum Geologists Bulletin v. 46, p. 2019–2032.

Berg, R. R., and Romberg, F. E., 1966, Gravity profile across the Wind River Mountains, Wyoming: Geological Society of America Bulletin, v. 77, p. 647–656.

Berryman, R. J., ms, 1942, The geology of the Deer Creek-Little Deer Creek area, Converse County, Wyoming: M.S. thesis, University of Wyoming, Laramie, Wyoming.
Blackstone, D. L., Jr., 1983, Laramide compressional tectonics, southeastern Wyoming: University of Wyoming Contributions to Geology, v. 22, p. 1–38.
Blythe, A. E., Sugar, A., and Phipps, S. P., 1988, Structural profiles of Ouachita Mountains, western Arkansas: American Association of Petroleum Geologists Bulletin v. 72, p. 810–819.
Braddock, W. A., Calvert, R. H., Gawarecki, S. J., Nutalaya, P., 1970, Geologic Map of the Masonville Quadrangle Larimer County, Colorado: United States Geological Survey Map GQ-832.
Brown, W. G., 1984, Basement involved tectonics—Foreland areas: American Association of Petroleum Geologists Continuing Education Course Note Series no. 26, 92 p.
———— 1988, Deformational style of Laramide uplifts in the Wyoming foreland, *in* Schmidt, C. J., and Perry, W. J., editors, Interaction of the Rocky Mountain Foreland and the Cordilleran Thrust Belt: Geological Society of America Memoir 171, p. 1–25.
Butler, K., and Schamel, S., 1988, Structure along the eastern margin of the Central Cordillera, Upper Magdalena Valley, Colombia: Journal of South American Earth Sciences, v. 1, p. 109–120.
Chester, J. S., and Chester, F. M., 1990, Fault-propagation folds above thrusts with constant dip: Journal of Structural Geology, v. 12, p. 903–910.
Chester, J. S., Logan, J. M., and Spang, J. H., 1991, Influence of layering and boundary conditions on fault-bend and fault-propagation folding: Geological Society of America Bulletin, v. 103, p. 1059–1072.
Choukroune, P., 1989, The ECORS Pyrenean deep seismic profile reflection data and the overall structure of an orogenic belt: Tectonics, v. 8, p. 23–39.
Cook, D. G., 1988, Balancing basement-cored folds of the Rocky Mountain foreland, *in* Schmidt, C. J., and Perry, W. J., editors, Interaction of the Rocky Mountain Foreland and the Cordilleran Thrust Belt: Geological Society of America Memoir 171, p. 53–64.
Colton, R. B., 1978, Geologic map of the Boulder-Fort Collins-Greeley area, Colorado: United States Geological Survey Miscellaneous Investigation Series Map I-855-G.
Cross, T. A., 1986, Tectonic controls of foreland basin subsidence and Laramide style deformation, western United States, *in* Allen, P. A., and Homewood, P., editors, Foreland Basins: Oxford, Blackwell, p. 15–39.
Cullins, H. L., 1969, Geologic map of the Mellen Hill Quadrangle, Rio Blanco and Moffat counties, Colorado: United States Geological Survey Geologic Quadrangle Map GQ-835.
Curry, W. H., and Curry, W. H., III, 1972, South Glenrock oil field, Wyoming: Prediscovery thinking and postdiscovery description, *in* R. E. King, editor, Stratigraphic Oil Fields—Classification, Exploration Methods, and Case Histories: American Association of Petroleum Geologists Memoir 16, p. 415–427.
Dengo, C. A., and Covey, M. C., 1993, Structure of the Eastern Cordillera of Colombia: Implications for trap styles and regional tectonics: American Association of Petroleum Geologists Bulletin, v. 77, p. 1315–1337.
Dibblee, T. W., 1982, Regional Geology of the Transverse Ranges Province of southern California, *in* Fife, D. L., and Minch, J. A., editors, Geology and Mineral Wealth of the California Transverse Ranges: South Coast Geological Society Guidebook No. 10, p. 7–26.
Dormorecki, J. W., ms, 1986, Integrated geophysical survey of the Golden thrust north of Golden, Colorado: M.S. thesis T3052, Colorado School of Mines, Golden, Colorado 134 p.
Erslev, E., 1991, Trishear fault-propagation folding: Geology, v. 19, p. 618–620.
Erslev, E., Rogers, J. L., and Harvey, M., 1988, The northeastern Front Range revisited: horizontal compression and crustal wedging in a classic locality for vertical tectonics, *in* Holden, G. S., editor, Geological Society America Field Trip Guide: Colorado School of Mines Professional Contributions 12, p. 122–133.
Eubank, R. T., and Makki, A. C., 1981, Structural Geology of the central Sumatra back-arc basin: Indonesian Petroleum Association, Annual Convention, 10th, Proceedings, p. 153–196.
Fraissinet, C., Zouine, W. M., Morel, J-L., Poisson, A., Andrieux, J., and Faure-Muret, A., 1988, Structural evolution of the southern and northern central High Atlas in Paleogene and Mio-Pliocene times, *in* Jacobshagen, V., editor, The Atlas System of Morocco: Berlin, Springer-Verlag, p. 273–291.

Froitzheim, N., Stets, J., and Wurster, P., 1988, Aspects of western High Atlas tectonics: *in* Jacobshagen, V., editor, The Atlas System of Morocco: Berlin, Springer-Verlag, p. 219–244.

Golombek, M. P., Plescia, J. B., and Franklin, B. J., 1991, Faulting and folding in the formation of planetary wrinkle ridges: Proceedings of Lunar and Planetary Science, v. 21, p. 679–693.

Golombek, M., Suppe, J., Narr, W., Plescia, J., and Banerdt, B., 1990, Does wrinkle ridge formation on Mars involve most of the lithosphere?: Lunar and Planetary Science, v. 21, p. 421–422.

Gries, R., 1983, Oil and gas prospecting beneath the Precambrian of foreland thrust plates in the Rocky Mountains: American Association of Petroleum Geologists Bulletin, v. 67, p. 1–26.

Gries, R., and Dyer, R. C., 1985, Seismic exploration of the Rocky Mountain Region: Rocky Mountain Association of Geologists and Denver Geophysical Society, Denver, 299 p.

Hansen, W. R., 1984, Letter in "Forum": Mountain Geologist, v. 21, p. 73.

Hennings, P. H., and Spang, J. H., 1987, Sequential development of Dry Fork Ridge anticline, northeastern Bighorn Mountains, Wyoming and Montana: University of Wyoming Contributions to Geology, v. 25, p. 73–93.

Hoppin, R. A., 1970, Structural Development of Five Springs Creek Area, Bighorn Mountains, Wyoming: Geological Society of America Bulletin, v. 81, p. 2403–2416.

Jackson, J., and Fitch, T., 1981, Basement faulting and the focal depths of the larger earthquakes in the Zagros mountains (Iran): Royal Astronomical Society Geophysical Journal, v. 64, p. 561–586.

Jamison, W. R., 1987, Geometric analysis of fold development in overthrust terranes: Journal of Structural Geology, v. 9, p. 207–219.

Julivert, M., 1970, Cover and basement tectonics in the Cordillera Oriental of Colombia, South America, and a comparison with some other folded chains: Geological Society of America Bulletin, v. 81, p. 3623–3646.

Kellogg, J. N., and Bonini, W. E., 1982, Subduction of the Caribbean plate and basement uplifts in the overriding South American plate: Tectonics, v. 1, p. 251–276.

Kerr, J. W., 1977, Cornwallis fold belt and the mechanism of basement uplift: Canadian Journal of Earth Sciences, v. 14, p. 1374–1401.

Lowell, J. D., 1985, Structural Styles in Petroleum Exploration: Tulsa, Oklahoma, Oil and Gas Consultants International Publications, 460 p.

Mallory, W. M., 1972, Pennsylvania arkose and the ancestral Rocky Mountains, *in* Mallory, W. M., editor, Geologic Atlas of the Rocky Mountain Region: Denver, Colorado, Rocky Mountain Association of Geologists, p. 121–132.

Matthews, V., III, editor, 1978, Laramide Folding Associated with Basement Block Faulting in the Western United States: Geological Society of America Memoir 151, 247 p.

———— 1986, A case for brittle deformation of the basement during the Laramide Revolution in the Rocky Mountain foreland province: Mountain Geologist, v. 23, p. 1–5.

McCaig, A., 1988, Vector analysis of fault bends and intersecting faults: Journal of Structural Geology, v. 10, p. 121–124.

McKenzie, D. P., and Morgan, W. J., 1969, Evolution of triple junctions: Nature v. 224, p. 125–133.

Medwedeff, D. A., ms, 1988, Structural Analysis and Tectonic Significance of Late-Tertiary and Quaternary, Compressive-Growth Folding, San Joaquin Valley, California: Ph.D. thesis, Princeton University, 184 p.

———— 1992, Geometry and kinematics of an active, laterally-propagating wedge thrust, Wheeler Ridge, California, *in* Mitra, S., and Fisher, G., editors, Structural Geology of Fold and Thrust Belts: Baltimore, Maryland, Johns Hopkins University Press, p. 3–28.

Meier, B., Schwander, M., and Laubscher, H. P., 1987, The tectonics of Tachira: a sample of north Andean tectonics, *in* Schaer, J.-P., and Rodgers, John, editors, The Anatomy of Mountain Ranges; Princeton, New Jersey, Princeton University Press, p. 229–237.

Mitra, S., 1993, Geometry and kinematic evolution of inversion structures: American Association of Petroleum Geologists Bulletin, v. 77, p. 1159–1191.

Molnar, P., and Chen, W-P., 1983, Seismicity and mountain building, in, Hsu, K., editor, Mountain Building Processes: Zurich, Switzerland, Academic Press, p. 41–57.

Mount, V. S., and Suppe, John, 1987, State of stress near the San Andreas fault: implications for wrench tectonics: Geology v. 15, p. 1143–1146.

Mount, V. S., Suppe, John, and Hook, S. C., 1990, A foreward modeling strategy for balancing cross sections: American Association of Petroleum Geologists Bulletin, v. 74, p. 521–521.

Myers, R. E., McCarthy, T. S., and Stanistreet, I. G., 1989, A tectono-sedimentary reconstruction of the development and evolution of the Witwatersrand basin, with particular emphasis on the central Rand Group: University of Witwatersrand Economic Geology Research Unit Information Circular no. 216, p.

Narr, Wayne, ms, 1990, Deformational Behavior and Kinematics of Basement-Involved Structures and Joint Spacing in Sedimentary Rocks: Ph.D. thesis, Princeton University, 243 p.

———— 1993, Deformation of basement in basement-involved, compressive structures, *in* Schmidt, C. J., Chase, R., and Erslev, E., editors, Laramide Basement Deformation in the Rocky Mountain Foreland of the Western United States: Geological Society of America Special Paper 280, p. 107–124.

Okulitch, A. V., Packard, J. J., and Zolnai, A. I., 1986, Evolution of the Boothia uplift, arctic Canada: Canadian Journal of Earth Sciences v. 23, p. 350–358.

Perry, W. J., Grout, M. A., Hainsworth, T. J., and Tang, R. L., 1988, Wedge model for late Laramide basement-involved thrusting, Grand Hogback monocline and White River uplift, western Colorado: Geological Society of America Annual Meeting. Abstracts with Programs, v. 20, p. A384.

Pierce, W. G., 1966, Geologic Map of the Cody Quadrangle, Park County, Wyoming: United States Geological Survey Geological Quadrangle Map GG-542.

Pierce, W. G., and Nelson, W. H., 1968, Geologic map of the Pat O'Hara Mountain Quadrangle, Park County, Wyoming: United States Geological Survey Geological Quadrangle Map GQ-755.

Powers, R. B., 1986, The Willow Creek fault, eastern Uinta Mountains—geologic analysis of a foreland subthrust play, *in* Stone, D. S., editor, New Interpretations of Northwest Colorado Geology: Denver, Colorado, Rocky Mountain Association Geology, p. 183–190.

Price, R. A., 1981, The cordilleran foreland thrust and fold belt in the southern Canadian Rocky Mountains, *in*, Coward, M. P., and McClay, K. R., editors, Thrust and Nappe Tectonics: Geological Society of London Special Publication n. 9, p. 427–448.

Prucha, J. J., Graham, J. A., and Nickelson, R. P., 1965, Basement controlled deformation in Wyoming Province of Rocky Mountain foreland: American Association of Petroleum Geologists v. 49, p. 966–992.

Ramsay, J. G., 1980, Shear zone geometry: a review: Journal of Structural Geology, v. 2, p. 83–99.

Ramsay, J. G., and Huber, M. I., 1987, The Techniques of Modern Structural Geology, Volume 2: Folds and Fractures: London, Academic Press, p. 309–700.

Robertson, P., and Burke, K., 1989, Evolution of Southern Caribbean Plate Boundary, Vicinity of Trinidad and Tobago: American Association of Petroleum Geologists Bulletin v. 73, p. 490–509.

Rodgers, John, 1987, Chains of basement uplifts within cratons marginal to orogenic belts: American Journal of Science, v. 287, p. 661–692.

Rowley, P. D., and Hansen, W. R., 1979, Geologic map of the Plug Hat Rock Quadrangle, Moffat County, Colorado: United States Geological Survey Geologic Quadrangle Map GQ-1514.

Rowley, P. D., Hansen, W. R., Tweto, O., and Carrara, P. E., 1985, Geologic map of the Vernal 1° × 2° quadrangle, Colorado, Utah, and Wyoming: United States Geological Survey Miscellaneous Investigation Series Map I-1526.

Sears, W. A., ms, 1949, Geology of the Deer Creek-Smith Creek area, Converse and Natrona Counties, Wyoming: M.S. thesis, University of Wyoming.

Sébrier, M., Mercier, J. L., Macharé, J., Bonnot, D., Cabrera, J., and Blanc, J. L., 1988, The state of stress in an overriding plate situated above a flat slab: the Andes of central Peru: Tectonics v. 7, p. 895–928.

Shaw, J. H., Bischke, R. E., and Suppe, John, 1994, Relationships between folding and faulting in the Loma Prieta epicentral zone: Strike-slip fault-bend folding, *in* The Loma Prieta, California, Earthquake of October 17, 1989: U.S. Geological Survey Professional Paper (in press).

Smithson, S. B., Brewer, J., Kaufman, S., Oliver, J., 1978, Nature of the Wind River thrust, Wyoming, from COCORP deep-reflection data and from gravity data: Geology, v. 6, p. 648–652.

Spang, J. H., Evans, J. P., and Berg, R. R., 1985, Balanced cross sections of small fold-thrust structures: Mountain Geologist v. 22, p. 41–46.

Stanley, R. S., and Armstrong, T. R., 1988, Palinspastic analysis of the Taconian hinterland as shown in the central Vermont transect: Geological Society of America Abstracts. with Programs, v. 20, p. A395.
Stearns, D. W., ms, 1970, Drape Folds Over Uplifted Basement Blocks with Emphasis on the Wyoming Province: Ph.D. thesis, Texas A&M University, 118 p.
———— 1971, Mechanisms of drape folding in the Wyoming Province, *in* Renfro, A. R., editor, Symposium on Wyoming Tectonics and their Economic Significance: Wyoming Geological Association, Annual Field Conference, 23rd, Guidebook, p. 125–143.
———— 1978, Faulting and forced folding in the Rocky Mountains foreland, *in* Matthews, V., III, editor, Laramide folding associated with basement block faulting in the western United States: Geological Society of America Memoir 151, p. 1–37.
Stearns, D. W., and Jamison, W. R., 1977, Deformation of sandstones over basement uplifts, Colorado National Monument, *in* Veal, H. K., editor, Exploration frontiers of the Central and Southern Rockies: Rocky Mountain Association of Geologists Guidebook, 1977, p. 31–39.
Stone, D. S., 1983, The Greybull Sandstone pool (Lower Cretaceous) on the Elk Basin thrust-fold complex, Wyoming and Montana, *in* Lowell, J. D., editor, Conference on Rocky Mountain Foreland Basins and Uplifts: Rocky Mountain Association of Geologists p. 345–356.
———— 1984, The Rattlesnake Mountain, Wyoming, debate: a review and critique of models: Mountain Geologist, v. 21, no. 2, p. 37–46.
———— 1986, Seismic and borehole evidence for important pre-Laramide faulting along the axial arch in northwest Colorado, *in* Stone, D. S., editor, New Interpretations of Northwest Colorado Geology; Denver, Colorado, Rocky Mountain Geological Association, p. 19–36.
Suppe, John, 1983, Geometry and kinematics of fault-bend folding: American Journal of Science, v. 283, p. 684–721.
———— 1985, Principles of Structural Geology: Englewood Cliffs, Prentice-Hall, Inc., 537 p.
———— 1986, Reactivated normal faults in the western Taiwan fold-and-thrust belt: Geological Society of China Memoir 7, p. 187–200.
Suppe, John, and Medwedeff, D. A., 1990, Geometry and kinematics of fault-propagation folding: Eclogae Geologicae Helvetiae v. 83, p. 409–454.
Suppe, John, and Narr, Wayne, 1989, Fault-related folding on the Earth with application to wrinkle ridges on Mars and the Moon: Tectonic Features on Mars, *in* Watters, T. R. and Golombeck, M. P., editors, MEVTV Workshop on Tectonic Features on Mars, Houston, Texas: Lunar and Planetary Institute Technical Report 89-06, p. 55–56.
Suppe, John, Chou, G. T., and Hook, S. C., 1991, Rates of folding and faulting determined from growth strata, *in* K. R. McKlay, editor, Thrust Tectonics: London, Chapman & Hall, p. 105–121.
Sylvester, A. G., and Smith, R. R., 1979, Structure section across the San Andreas fault zone, Mecca Hills, *in* Crowell, J. C., and Sylvester, A. G., editors, Tectonics of the juncture between the San Andreas fault system and the Salton Trough, southeastern California: University of California, Santa Barbara, Department of Geological Sciences, p. 125–139.
Tapponier, P., and Molnar, P., 1979, Active faulting and Cenozoic tectonics of the Tien Shan, Mongolia, and Baykal regions: Journal of Geophysical Research, v. 84, p. 3425–3459.
Thom, W. T., Jr., 1955, Wedge uplifts and their tectonic significance, *in* Poldervaart, A., editor, Crust of the Earth: Geological Society of America Special Paper 62, p. 369–375.
Trumpy, R., 1980, An Outline of the Geology of Switzerland: Basel, Wepf & Co., 104 p.
Watkinson, A. J., 1993, A footwall system of faults associated with a foreland thrust in Montana: Journal of Structural Geology, v. 15, p. 335–342.
Wells, A. T., Moss, F. J., and Sabitay, A., 1972, The Ngalia Basin, Northern Territory—Recent geological and geophysical information upgrades petroleum prospects: Australian Petroleum Exploration Association Journal, p. 144–152.
Williams, G. D., and Fischer, M. W., 1984, A balanced section across the Pyrenean orogenic belt: Tectonics, v. 3, p. 773–780.
Wise, D. U., 1963, Keystone faulting and gravity sliding driven by basement uplift of Owl Creek Mountains, Wyoming: American Association of Petroleum Geologists Bulletin v. 47, p. 586–598.
———— 1964, Microjointing in Basement, middle Rocky Mountains of Montana and Wyoming: Geological Society of America Bulletin, v. 75, p. 287–306.
Xiao, H., and Suppe, John, 1992, Origin of rollover: American Association of Petroleum Geologists Bulletin, v. 76, p. 509–529.